Team Minion's Design and Competition Approach for the 2026 Maritime RobotX Challenge

Bharat Jagwani, Sarthak Aggarwal, Sagar Sarkar, Sean Johnson, Willis Proper, Mateus Prudencio, Jacob Young, Nam Tran, Luke Coblentz, Joshua Wenger, Alexander Kilian, Amaya Baker, Mason Cisco, Myles Abram, Quinn Isaksen, Dr. Eric Coyle, Dr. Patrick Currier

***Abstract*—Embry-Riddle Aeronautical University's Team Minion enters the 2026 Maritime RobotX Challenge with the *Minion Fleet*, a multi-domain System-of-Systems comprising an Uncrewed Surface Vehicle (USV), an Uncrewed Aerial Vehicle (UAV), and an Uncrewed Underwater Vehicle (UUV). Junior, a quarter-scale USV, serves as the mothership for perception, communications, and decision-making. Kevin, a heavy-lift UAV with a sealed electrical system and a wire-based capture mechanism, and JIT, a bi-modal UUV built on a modified BlueROV2 Heavy, complete the fleet. Development follows the team's *Minion Process*, a flexible systems engineering framework that balances academic, research, and competition needs. A two-link radio architecture complies with Singapore spectrum regulations while preserving platform autonomy. Testing progresses from computer-aided analysis and bench testing to platform integration and field testing, supported by a multi-vehicle simulation environment. Finally, each competition task is decomposed into vehicle-level capabilities, and team confidence in each is combined into a ranked task priority list executed by the fleet's task manager.**

I. Overview

TEAM Minion is an interdisciplinary team of undergraduate and graduate students from Embry-Riddle Aeronautical University (ERAU). In addition to competing in the Maritime RobotX Challenge, the uncrewed systems are used to provide graduate research and undergraduate experiential learning opportunities. As such, the strategy of Team Minion is to create tools and resources that balance the academic, research, and competition needs of its members. This has led Team Minion to develop a systems-based design, where uncrewed systems and software modules are primarily developed for research or academic purposes, then adapted to the competition tasks to maximize competition performance. This paper will highlight how Team Minion's design strategy has led to the Minion Fleet, a multi-domain team of connected systems, how team Minion's testing strategy ensures robustness and competition compliance, and how testing demonstrates capabilities that map to 2026 Maritime RobotX Competition tasks.

II. Competition Strategy: The Vision

The 2026 competition marks a major shift from Team Minion's 2024 approach, requiring coordinated USV, UAV, and UUV operation. With Minion (the 2014–2024 USV) no longer eligible, the UAV reaching end-of-life, and almost no UUV experience, developing three new mature platforms within one year was impractical. Team Minion instead leveraged existing synergistic research, academic, and competition work already advancing UxV technology, adding new capability only where the benefit justified the risk. This let the team keep progressing while RoboNation's detailed task and scoring information was still pending, and meant task/level selection (Core, Advanced, Disruptive) would be driven by demonstrated system maturity rather than a fixed target.

Junior, a roughly quarter-scale derivative of Minion originally built for research and RoboBoat, was three months into development when RobotX 2026 was announced. It retained Minion's proven autonomy, perception, navigation, controls, electrical, and communications approaches, so repurposing it for RobotX required minimal hardware changes. This was the lowest-risk path to rebuilding USV capability.

Noodle, the prior UAV, had performed reliably at RobotX 2022 and 2024 but lacked the flight time and capture mechanisms for full task completion. The team retired it from active development (keeping it as a flight-ready backup) and shifted focus to Kevin, a new heavy-lift endurance aircraft designed as a long-term research platform capable of completing the Infrastructure Survey and Repair and Coordinated Logistics tasks even at the Disruptive level. Noodle's continued flight-readiness offset the added risk of focusing on the newer Kevin.

The UUV was the team's largest gap, since Team Minion had no UUV capable of the 2026 tasks. A collaboration with Embry-Riddle's RoboSub team was considered but dropped as too disruptive to their own transition. Instead, the team used RoboNation grant funding to acquire a BlueROV2 Heavy, named JIT, for bimodal operation: a periscope with GPS and communications for near-surface work, and a DVL for untethered submerged operation. Both modes rely on waypoint navigation, an area where the team already had USV/UAV experience.

Together, Junior, Kevin, Noodle, and JIT form a System of Systems (SoS) meant to cover the full mission set while limiting development risk, with Junior, the most capable platform, acting as mothership and issuing commands to the others. Section III-F describes how the SoS architecture shares data and executes mission tasks.

The paper proceeds with design strategy and outcomes (Section III), testing strategy and results (Section IV), and task/capability-level prioritization based on demonstrated reliability and readiness (Section V).

III. Design Strategy

A. Philosophy

Team Minion is rooted in a SoS design philosophy, where modular hardware and software tools are developed that can be re-configured to achieve complex missions at competition and for research purposes.

When developing a new tool, Team Minion utilizes the following evaluation criteria as the basis of its engineering philosophy:

- **Safety** of personnel, the vehicles, and the environment are a top priority. This is directly reflected in every step of the design process through redundancy in critical systems and improved visual aids for system monitoring.
- **Modularity** makes the system elements interchangeable across platforms, allowing for rapid integration and testing. Tools are initially developed at base-level capability and expanded as time and resources allow for improved capability.
- **Performance** focused development is used to evaluate the level of performance each system can achieve. Each sub-system has its own performance metrics and targets.
- **Novelty** is sought as a means to provide research opportunities and exceed capabilities of its competitors, but novelty must be balanced with anticipated performance and safety.

B. Systems Engineering

The strategic vision for the competition is incorporated into the team's unique systems engineering process, called Minion Process, shown in Fig. 1. Minion Process utilizes traditional systems engineering sub-processes starting with a mapping of competition tasks, academic interests, and research goals to design requirements. These design requirements are distributed to Team Minion's sub-teams, organized by vehicle (USV, UUV, UAV), and form the foundation of brainstorming, conceptual design and sub-team decision-making. Software tools, such as ANSYS, are used to evaluate the design and verify compliance with the established criteria. A formal design review follows with team advisors and members of the other sub-teams. This review can send the design back into any of the prior stages, or approve fabrication if all parties are satisfied. When rejecting, an appropriate stage of Minion process to return the design to is determined. For instance, if new criteria is established the design may need to return to requirements definition.

The key differences in Minion Process and several well-known systems engineering approaches, such as Agile [1] and Scrum [2], is the flexible timing and ability to send the design back to prior steps from any stage of the process. As such, Minion Process enables the completion of tasks that vary in complexity, scope, and objective, often according to non-linear timelines. For example, the timelines associated with a course or graduate research project may differ significantly from those undertaken by a volunteer team. Furthermore, changes to competition in the form of handbook updates [4] may require a design to return to an earlier stage of Minion Process. Regardless of the timeline or number of iterations, all sub-processes are completed before finalization.

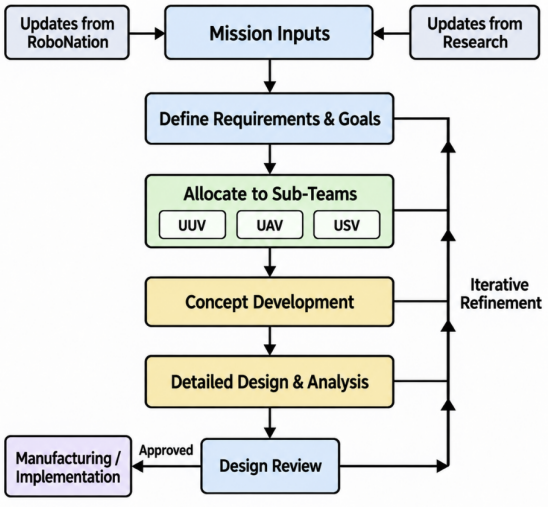


Fig. 1: Systems Engineering Adaptation: Minion Process

With the move to a true multi-domain competition, the outcome of Minion Process is best organized by operating domain. For each domain vehicle (USV, UAV, and UUV), the design goals, a brief description of the design outcome, and outcome novelty are discussed below.

C. Junior, the USV Mothership

Design Goals: Junior, shown in Fig. 2, was originally designed as a smaller surrogate to the WAM-V for the purpose of easier testing and to compete in RoboBoat 2026 [9]. The goal for RobotX 2026 is to transform Junior into the central authority within the Minion Fleet, or in other words be a 'mothership' for perception, communications, and decision-making. As such, the mothership must be able to stay on-station for extended periods of time. It must also be constantly aware of its surroundings and the operations of the UAV and UUV. This led to explicit RobotX 2026 goals for Junior of:

- Hydrodynamic rigid pontoons for low-drag and predictable behavior
- Omni-directional surge, sway and yaw control with $\pm 20cm$ and $\pm 3°$ error
- Object and color identification to $20m$ off vessel bow
- Minimum 40% bandwidth and computing overhead for UAV and UUV cooperation

System Description: Long pontoons with a round cross-section were selected to raise the draft line, resulting in lower drag and improved water flow over V-shape and flat-bottom hull designs. To create the round shape, the pontoons' construction consists of low-porosity insulation foam cut by a water jet with rigid wooden dowel spines. Pontoon fronts are capped with a 3D printed nose cone and thruster mounts are inserted through the rear of the pontoons for improved stability over mounting at the end of the pontoon. All surfaces were wrapped in a fiberglass skin and T-slot rails are affixed to the top and bottom for modular mounting of in-water sensing (future objective) and the platform deck to set platform trim

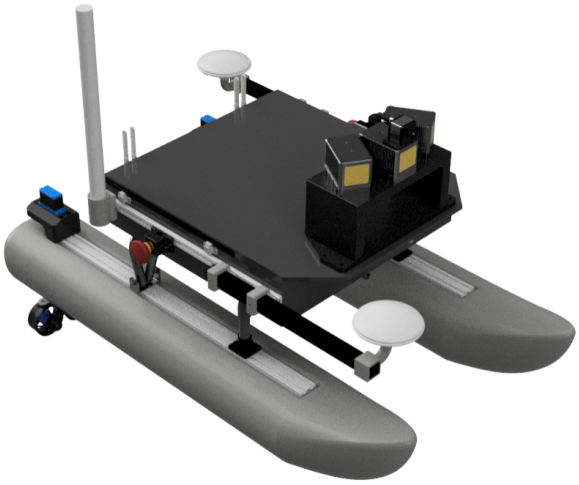


Fig. 2: Junior USV Design

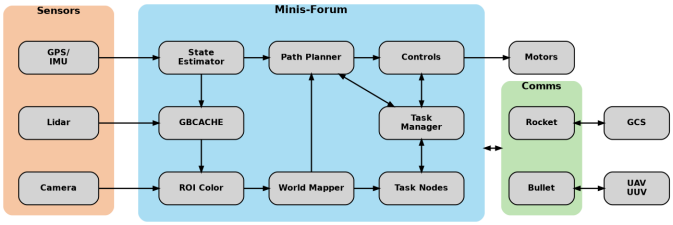


Fig. 3: Junior Software Architecture

to a desired 1-2 degrees. To achieve omni-directional control, Junior is equipped with two Blue Robotics T200 thruster pairs that are yaw-actuated using Hitec 845WP waterproof servos having a range of $\pm 90°$.

As the brains of the Minion Fleet, Junior has the most intensive sensor suite (compared to the UAV and UUV) to perform the bulk of world map generation and tasking decisions. Three Livox Horizon units produce dense point clouds in a forward 165°FOV that are processed using the GB-CACHE [5] algorithm for object extraction. A 65° FOV high-dynamic range (HDR) camera is used for object color classifications based on regions-of-interest flagged by the LiDARs. This perception suite replicates the capabilities of the WAM-V. A JAVAD DELTA-DI GNSS/IMU provides detailed localization allowing for fine control and the building of one global world map for decision-making. Observed objects continuously populate the world map, where path planning and tasking logic are applied and executed. Base station remote access is accomplished over a Ubiquiti Rocket while autonomous communications with the Minion Fleet are done over a Ubiquiti Bullet, allowing for each to be under separate frequencies for radio frequency compliance in Singapore. Furthermore, the MINISFORUM MS-01 Core i9-13900H computer and companion graphics card provided almost double the computing power required by Junior. These communication and computing resources therefore give Junior the overhead capability to perform true Mothership operations of centralized computing and message routing.

Software Architecture: Junior's software architecture, shown in Fig. 3, is nearly identical to its predecessor, Minion. This architecture uses a modular set of sub-routines for State Estimation, Object Detection/Classification (GB-CACHE and ROI Color Extraction), Path Planning, Controls, and Tasking (Task Manager). Using ROS2's Data Distribution Service (DDS), each process publishes and subscribes to the information it requires from other modules and outputs standardized message types for downstream processing. Minion's software routines include multiple published methodologies, including GB-CACHE for Object Detection and Classification [5], an Anytime Visibility-Voronoi Path Planner [7], and a patent-pending control allocation system [10]. These are original works by team Minion, its alumni, and advisors.

Perhaps the most important decision Junior must make is which competition task or sub-task should have operational authority of the Minion Fleet. This decision is made by the task manager, called MinionTask. Tasks and sub-tasks are programmed into independent processes composed of two parts: a routine to identify if starting conditions are met (such as identify key objects or completion of a different sub-process of the task), and a state machine to execute behaviors. The status of the task's starting condition is broadcast as a ROS2 topic to MinionTask. Using a task priority set by the team, MinionTask selects the best task among those that are available for execution and publishes the task that has operational authority to all three vehicles. Only when authority has been given will the vehicles respond to commands from the individual tasks. Most task state machines follow a process of select behavior, plan behavior, execute behavior until complete, and repeat until all behaviors complete. More information about the task manager is given in the *Competition Strategy*, section V.

Novelty:

Junior includes many novel concepts, starting with the novel "patent-pending" controls approach. Demonstrated in RobotX'24 on the WAM-V, the holonomic control allocation method was refined for Junior for this competition. This controls approach allows full control authority with independent Surge, Sway and Yaw control using inverse kinematics and a real time decision-tree based solver providing the most efficient commmands optimized for maximum control authority[10].

Next is the pontoon design. Here, aluminum t-slot rails along the pontoons and deck allow for re-configuration of the vessel as mission requirements change. The deck rails allow for adding and re-configuring components, while the pontoon rails allow for re-balancing the boat as payload distribution changes. There are even rails under the pontoons to mount underwater sensing payloads in the future. These rails also enable fast tear-down and set-up which will be necessary for shipping to competition, reducing the team's logistic issues.

Meanwhile, the instrument deck boasts ultra-lightweight aircraft-grade aluminum honeycomb panels. At 5 lbs empty, it is a third of the weight compared to alternative solid material designs. This is extremely helpful in reducing the drag of the system by having less draft in the water.

Next, the entire system can run on one or two 18V drill batteries that are configured electrically to provide hot-swapping

capability. This means that a new battery can be inserted without shutting off the system and provide theoretically infinite runtime. These two ports also double the runtime of a single charge. The batteries can also be locally sourced, including via Singaporean vendors. These batteries also improve safety by using a safer chemistry, durable packaging, and built-in Battery Management Systems (BMS) that are often not found in typical hobby grade batteries.

Finally, harsh sunlight and glare from the water surface can create unruly contrast in the camera image. To combat this, Junior's camera is equipped with a polarized filter and hardware-level high dynamic range imagery, bolstering color detection under poor or high lighting conditions. Junior's triple Livox Horizon sensors produce significantly more detail on object profiles than the typical repeating-pattern LiDAR sensors, as shown in Fig. 4.

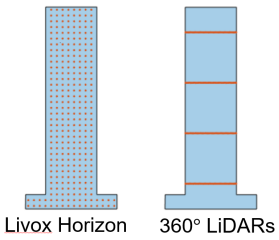


Fig. 4: LiDAR point density comparison for a traditional scanning LiDAR and a single Livox Horizon Unit on a simulated buoy. Each orange point is an estimated LiDAR return.

D. Kevin, the worker UAV

Design Goals: A primary objective of the UAV design is to be the heavy lift companion for Junior, capable of carrying a capture mechanism, more capable sensors, and future research payloads. The system should also last for the next four years (through RobotX 2030), to minimize costs and focus on refinement in future RobotX cycles. As such, its most important design goals include:

- Continuous flight time of at least 30 minutes
- Capable of capturing, holding, and releasing the tin
- Survive an uncontrolled landing on water from 1m altitude
- Float for 1 hour before recovery without damaging the electrical components
- Carry optics and ranging to detect competition objects at altitudes of 5-20m
- Have a 4-year lifespan

System Description: Kevin, whose render is shown in Fig. 5, is primarily constructed using carbon fiber and 3D printed components to balance long-term robustness and repairability. Kevin uses the CUAV+Pixhawk V6X V2 flight controller, which is the same proven autopilot eco-system as its predecessor. For localization, the UAV uses the Neo 3 GPS antenna along with the Pixhawk's built in GPS receiver and IMU (Inertial Measurement Unit). For perception, Kevin utilizes an e-CAM86_CUONX camera with an FOV of $110°$ and a Robosense Airy LiDAR which has a FOV of $360° \times 90°$.



Fig. 5: Kevin UAV Design

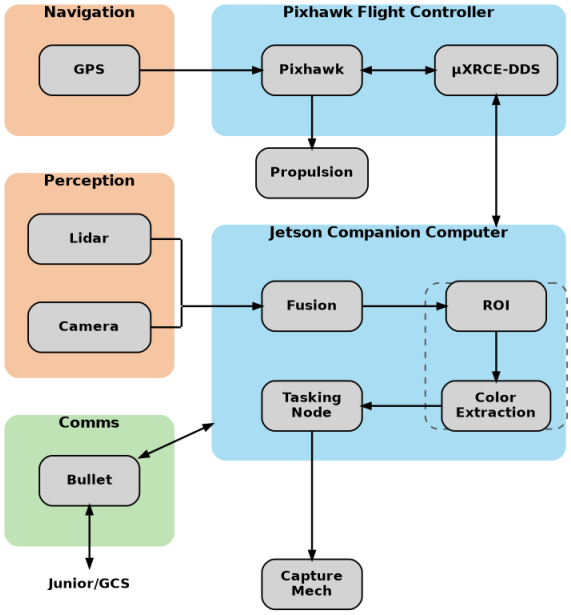


Fig. 6: Kevin Software Architecture

For propulsion, the UAV has 4 T-Motor U5 400kV brushless DC motors and 4 T-Motor ALPHA 40A ESCs with 16×5.4 Propellers, for a payload capacity of 11 kg. Kevin uses two Auline S70 Lithium Ion Batteries in a 6S4P configuration for power, which gives an estimated 35 minutes of operation when fully loaded. For storing all of the electronics, Kevin uses an internal rack mounted on 3d printed rails that can be easily removed from the main drone shell for battery removal compliance with the RobotX rules.

Software Architecture: The UAV relies heavily on its onboard CUAV flight controller, which runs the PX4 autopilot, for navigation and control. Its camera and LiDAR perception suite give the vehicle the sensing modality it needs to perceive its surroundings. Using sensor fusion, the UAV detects objects and extracts their color. This processed data is used to compute destination waypoints, which are sent to the flight controller to execute the flight maneuvers needed to reach the target. In the previous competition cycle, the UAV relied on camera data alone to guide precision landing; with the addition of lidar this cycle, both object detection and landing accuracy have improved.

Novelty: Kevin utilizes a unique capture mechanism, mod-

eled after Latching End Effector (LEE) [8], for the Survey and Repair and the Coordinated Logistics tasks. This system uses a wire mechanism to provide clamping force around the object that conforms from a single actuator. Kevin also differs from many competition UAVs by using a fully waterproof electrical system. Instead of exposed electronics that would likely be heavily damaged in a water landing, all major electrical components are sealed off inside of the carbon fiber shell in Kevin using a system of O-rings and D-channel gaskets. The use of a LiDAR for perception is also unique, in that it is not fully reliant on ambient lighting to detect landing areas and tins (though tin color still requires the camera sensor).

E. JIT, the bi-modal UUV

Design Goals: At a high level, the primary UUV goals were to minimize development time through commercial-off-the-shelf (COTS) solutions, ensure the system can operate in dark water, and can accept inputs from Junior, the USV Mothership. Given the increased risk of developing a new modality, the team also wanted to ensure even if the UUV was unable to complete competition tasks, it would record sufficient data to trouble-shoot the issues that arose. This led to specific design goals of:

- Surface and sub-surface waypoint following (i.e. Bi-Modal Operation) to $\pm 1m$
- Wireless surface communication with Junior and RC operator
- Fail-safe surfacing
- Vision and SONAR Logging of the pipeline



Fig. 7: JIT UUV Design

System Description: The UUV solution, known as JIT and shown in Fig. 7, started as a Blue Robotics BlueROV2 Heavy which was acquired with RoboNation grant support. But to support the additional sensors and computing needs, a secondary electronics enclosure has been added and the vehicle operates inverted to improve roll stability. This inversion puts the new tube enclosure, which is highly buoyant, high on the vehicle and also lowers the Z-axis thrusters further into the water when floating. JIT operates in two modes, surface and submerged, and stable control in both was a priority. Without the inversion, surface mode placed the thrusters within one inch of the waterline and cavitation occurs, where operating inverted prevents this inefficiency. For communication with the Junior USV and the RC operator, a periscope was constructed to house wireless communication equipment and a GPS locator. As such, JIT does not operate using a tether to the USV or RC operator. While the GPS provides location at the surface, a Water Linked A50 Doppler Velocity Log (DVL) is used for underwater localization.

JIT's E-stop system fails safe electrically in compliance with the competition rules. A normally-open relay is used cut power to all thrusters upon e-stop button, wireless, or lost communication conditions. As JIT is positively buoyant, the system will simply float to the surface under this condition. In software, a main health-monitor node can also open the relay and initiate a failsafe if an undesired condition, such as low battery voltage, occurs while submerged and not in contact with its operator or Junior. The UUV also detects when a planned maneuver would block that communication and will not trigger a fail-safe condition due to loss of communications under this condition.

Team Minion is generally unable to test JIT in dark water environments, as the team is not allowed to deploy underwater objects in its local waterways, thus all local testing was done in a recreational pool. As such, competition-like visibility could not be replicated and all competition data would be highly valuable and must be logged locally on JIT due to the aforementioned communications dropout. JIT is equipped with a Blue Robotics Ping 360 sonar for object awareness and an Omniscan FS450 side-scan sonar for detection of objects near the operating floor. Furthermore, a low-light HD USB camera is used to provide short-range visible context. Raw data from the perception and localization sensors is logged on a Raspberry Pi computer, known as the companion computer, which also handles communications with Junior, and is separate from the computer that JIT uses for navigation.

Software Architecture:

The stock BlueROV2 controls system uses BlueOS on a Raspberry Pi 4B and ArduSub on a BlueROV Navigator board to handle low-level control and state estimation. But this set-up does not natively support the ROS2 architecture needed for communication with Junior and bench testing showed the Raspberry Pi 4B computer to be nearly maximizing its processing power. To address this, a second Raspberry Pi 4B, running Ubuntu 22.04 and ROS 2 Humble, was added as a companion computer. In total this architecture gives us three compute blocks: the Navigator board (ArduSub), BlueOS (MAVLink router), and the ROS 2 computer. BlueOS connects to the companion computer over a MAVLink endpoint, and MAVROS exposes ArduSub's telemetry, state, and services as ROS 2 topics. Since JIT's position estimates come from integrating DVL velocity when submerged, error grows steadily over time, but was tested to be 10 cm in 5 minutes, which is less than the $\pm 1m$ requirement. The companion computer also runs a Ping360 scanning sonar for mapping objects in the water column.

Commands flow from the companion computer starting with input from an operator via an ExpressLRS (ELRS) receiver. The operator can choose manual commands for JIT, or set the

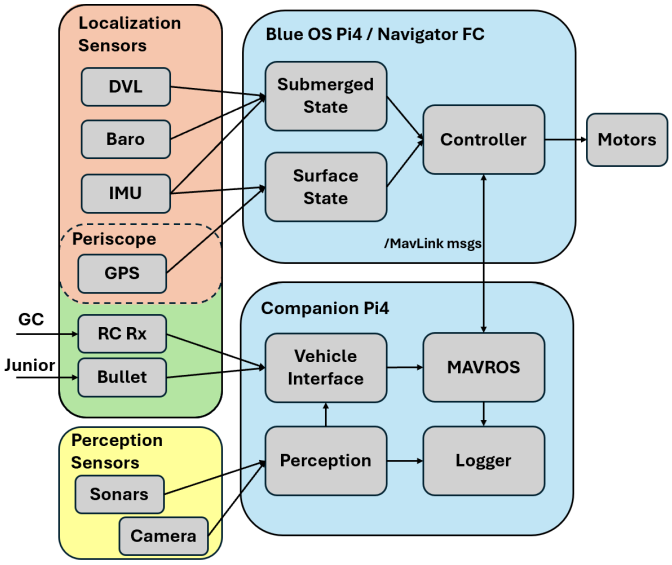


Fig. 8: JIT Software Architecture

vehicle into the failsafe or autonomous modes. Surface (GPS waypoints) and submerged (DVL pose) locomotion share one pipeline: both publish setpoints, but only one node, the vehicle interface, is allowed to write to MAVROS. It picks which position source is active and updates the desired waypoint when the mode or location changes. This lets ArduSub then execute the path on its own, but the check for waypoint completion is handled by the companion computer. On top of this sits the safety block, which provides a wireless update via a ROS topic on the health status of the UUV, including all faults that have been detected. If a fault occurs, it opens the relay contacts to trigger a failsafe. This gives the vehicle two ways to stop: a software disarm command sent through MavROS (confirmed by ArduSub's reported state) and a hardware power cut (reserved for real faults).

Novelty: JIT's primary innovation is its wireless bi-modal operation strategy. This prevents the issues the team experienced in the 2018 RobotX competition [3], where difficulty managing the tether was encountered and ultimately resulted in the UUV not participating in the competition. Additionally, Junior is significantly smaller than the WAM-V platform and would have issues with just integrating a tether management system.

On the surface, JIT communicates with the USV to receive tasking commands and utilizes onboard GNSS sensors for long term surface localization. A radio communication periscope packages a 5Ghz Ubiquiti Bullet, a 2.4GHz RC link, and a GNSS receiver in a depth-rated waterproof enclosure mounted to keep the antennas clear of the water in surfaced operation. As an acoustic modem was not within the team's budget this does mean that inter-vehicle communications are lost during submersion. At the task location(s), JIT submerges and relies on DVL-backed dead reckoning for localization. To allow for this submerged operation, the JIT also uses a clever strategy of detecting submersion to determine when to enforce the competition-required RC communication failsafes that must only be active at the surface.

F. System of Systems Approach

A key element of Team Minion's SoS approach is communications, for which Team Minion relies on radio frequencies. The system was built for US FCC limits, which are comparatively permissive. Singapore's stricter spectrum and power rules forced the team to change settings, but not a reconfiguration. The USV, UAV, and UUV each operate independently, so the architecture had to unite all three on one network without compromising any platform's autonomy or the team's control over each robot.

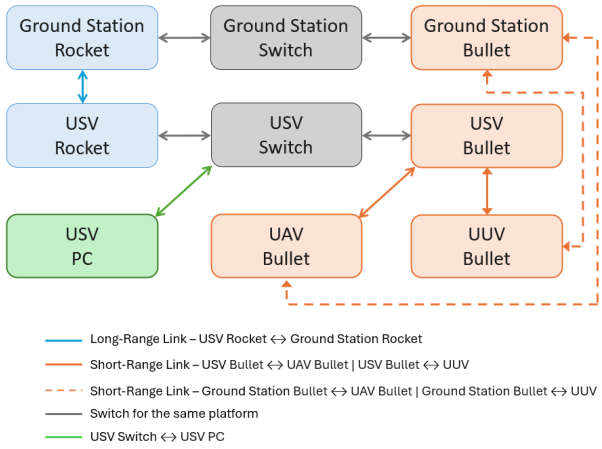


Fig. 9: SoS Hardware Communication Layer

The Ubiquiti Bullets used on Kevin and JIT don't support dynamic frequency selection (DFS), which is required for high power operation in Singapore, so they are restricted to lower power at competition. However, keeping the Bullet form factor was important, since fitting a larger Ubiquiti Rocket on the UAV and USV would have required significant hardware changes on both platforms. That constraint, combined with the need to remain compliant with Singapore's regulations, shaped the architecture into two links:

- **High-power link** (5500 MHz, 1000 mW, DFS channel): long-range link between the USV and ground station, where distance requires the extra power.
- **Low-power link** (5200 MHz, 100 mW, non-DFS channel): short-range link to connect the USV to the UAV and UUV, compliant with Singapore's local limits.

Both links bridge at IP Layer 2 through an unmanaged network switch on the USV, so every platform sits on one subnet and commands relay across the network with no routing overhead. The ground station includes both high power and low-power connections, so the UAV and UUV stay on the network during dockside standby, when they are far from the USV but close to the ground station. The UAV and UUV both roam between the USV and ground station radios automatically, connecting to whichever has the stronger signal. Co-channel interference is minimized by the separation difference between the USV and ground station. This SoS architecture is shown in Fig. 9.

The SoS uses the described communication architecture as their hardware layer, to share required system level and task level information. But ROS2 topics serve as the software layer,

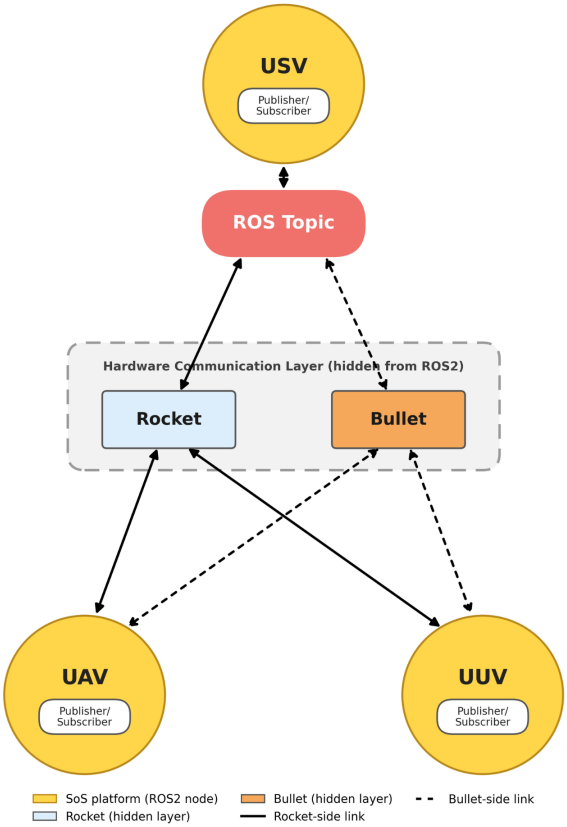


Fig. 10: SoS Software Communication Layer

to send information between platforms. The Fig. 10, shows an example of system level data sharing, with each vehicle publishing and subscribing to heartbeat topics, which follows the same layout as the RoboCommand Heartbeat message.

In addition to system level data, each vehicle also publishes and subscribes to task level information, which allows the SoS to coordinate behavior across the fleet rather than simply monitor individual vehicle status. Task level messages carry information such as current task assignment, task state (e.g., waiting, in-progress, complete), and any parameters required to execute the task (e.g., target waypoint, target ID).

IV. Testing Strategy

Team Minion emphasizes testing of both UxV hardware and software. Testing is divided into hardware and software strategies, with additional considerations for UAV testing. Each uses a tiered approach focused on safety, performance, and efficient use of team resources.

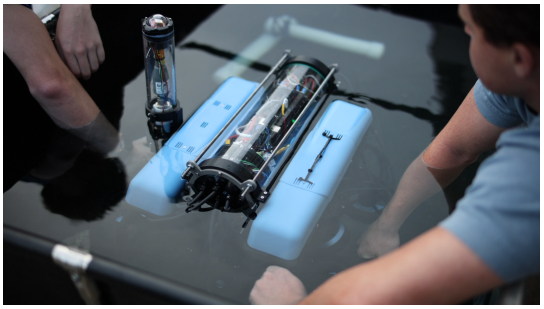
A. USV and UUV Hardware Testing Strategy

Team Minion uses an incremental hardware testing strategy refined over its previous RobotX competition cycles. For Junior and JIT, testing begins with low-risk analytical and component-level evaluation before progressing to platform integration and field testing. This approach identifies failures early, limits vehicle downtime, and reduces the risk of completed systems not meeting expectations. The four primary stages are:

1) **Computer-Aided Analysis** evaluates designs prior to fabrication. Fusion 360 is used to verify component interfaces, packaging, and system fit, while ANSYS is used for structural finite element analysis under static and dynamic loading conditions. Buoyancy calculations and circuit simulations are also performed where applicable to verify mechanical and electrical performance before hardware is produced.
2) **Bench Testing** evaluates individual components and subsystem prototypes before vehicle integration. Additive manufacturing is frequently used to rapidly produce prototype components for evaluating form, fit, and basic functionality before committing to more time- or resource-intensive fabrication methods. Basic functional testing then verifies intended operation, mechanical and electrical interfaces, sensor data, actuator response, and safety-critical functions in a controlled environment. Where practical, components are tested beyond nominal operating conditions to identify failure modes and performance limits. Results are used to refine the prototype, proceed to final fabrication, or return the design to an earlier development stage through Minion Process before full-platform integration.
3) **Platform Integration** combines validated hardware on Junior or JIT. Mechanical installation is followed by electrical, communication, sensor, software-interface, and control-system checks. Integration typically requires two to six weeks depending on system complexity and availability of team resources. Following installation, in-lab functional and safety checks verify that new systems operate correctly with the existing platform before field testing begins.
4) **Field Testing** evaluates the integrated platform in an operationally relevant environment. Junior and JIT testing progresses through inflatable pools (see Fig. 11a), shallow-water environments (see Fig. 11b), and open-water testing as appropriate for the system being evaluated. Each test identifies one or more specific objectives, the method used to evaluate them, the required test environment, and success or failure criteria. Results and anomalies are recorded and used to guide subsequent design or testing iterations.

USV and UUV field testing generally requires an RC driver, dock hand, and ground-station operator, with additional personnel added as required by the test environment or availability. Physical and RC emergency-stop methods are all verified before testing in public environments. Additionally, specific procedures are followed based on potential risks of each system. Examples of this include regularly checking for water ingress and battery status. Testing frequency scales with the competition calendar: early on, it's scheduled as-needed around new subsystem development, while closer to competition it becomes structured around shipping deadlines to leave time for corrective iterations, integration, and reliability testing.

A representative test plan and results are provided in Appendix A. The test plan documents the test objective, platform



(a) UUV JIT ingress testing on 09/12/2026



(b) USV controls test on 08/24/2026



(c) UAV Kevin manual flight stability test on 9/18/26

Fig. 11: System Field Tests

configuration, required environment, evaluation method, success criteria, observations, and any anomalies identified during testing.

B. Software

In the two prior competition cycles, Team Minion has relied on the VRX-supported simulation [6] of the WAM-V to evaluate its perception, autonomy, and decision-making software. With the transition to a multi-domain competition in 2026, significant effort was placed on adapting this environment to simulate a smaller USV, as well as the UAV and UUV. Ultimately, team Minion created a world that is representative of the 2026 RobotX tasks (see Fig. 12), which also allows for independent control and testing of each UxV. By first testing all software in the simulated environment, the team is able to address major issues prior to field testing the UxV systems and reserve critical in-water and flight time to tune for real-world conditions instead of debugging and testing of software logic.

An in-lab software shakedown is conducted the day before field testing to verify recent changes and ensure compatibility between the modified code and prior iteration. This process minimizes the risk of wasting valuable testing time and good weather windows while fixing compatibility issues. The shakedown involves key checks of updating vehicle code, successful code compilation, ensuring all dependencies are installed, confirming the responsiveness of the propulsion systems, checking node execution, and verifying system communications. Because of the logistic burden of in-water testing, there is a general expectation of at least three separate test objectives, or a key competition deadline, before a test is scheduled. Vehicles may operate via remote control or autonomous modes during software testing, but RC driver is always ready to take over autonomous operation.

ROS bag files are used to capture all sensor data and inter-algorithm communication during testing. These bags can be used later for performance assessment, and algorithm testing by treating the recorded data as live observations. The team uses a Network Attached Storage, NAS, to store the collected data, for easier accessibility. Following each test, the team conducts a debrief involving all present members. The debrief covers the key accomplishments from the test, as well as any issues or tasks that need to be addressed for the next test. These discussions serve as the starting point for planning the next testing cycle, helping to ensure the team stays focused on improvements and preparations for future tests.

C. UAV

Separate testing procedures also apply to UAV testing due to the inherent risks of operating over water and near people. As previously noted, the team utilized the simulation environment extensively during the development phase to test and validate the software for autonomous tasks. This approach significantly minimized the risk of accidental crashes during real-world testing. To further ensure the safety of the pilot and crew members, as well as to mitigate risk, multiple checklists were created which have been submitted as part of the Proof of Readiness submission. These include:

- Manual Flight Readiness Checklist
- Pre-Flight Report
- Regular Manual Flight Checklist
- Manual Flight Checklist
- Crash and Failed Test Checklist

Depending on the type of test being conducted, the relevant checklist is consulted before the test begins and after it is completed, ensuring safety protocols are maintained and all necessary steps are followed.

Tests are conducted in a netted enclosure measuring approximately 50 ft x 50 ft x 30 ft (see Fig. 11c), except when over-water testing is required. This enclosed space allows for safe and controlled testing of the UAV by minimizing risk of environmental interference or accidents. For testing over water, which is a public area, the UAV team needed to obtain permission from a University Safety Review Board (SRB) and the local authority. To gain these permissions Team Minion

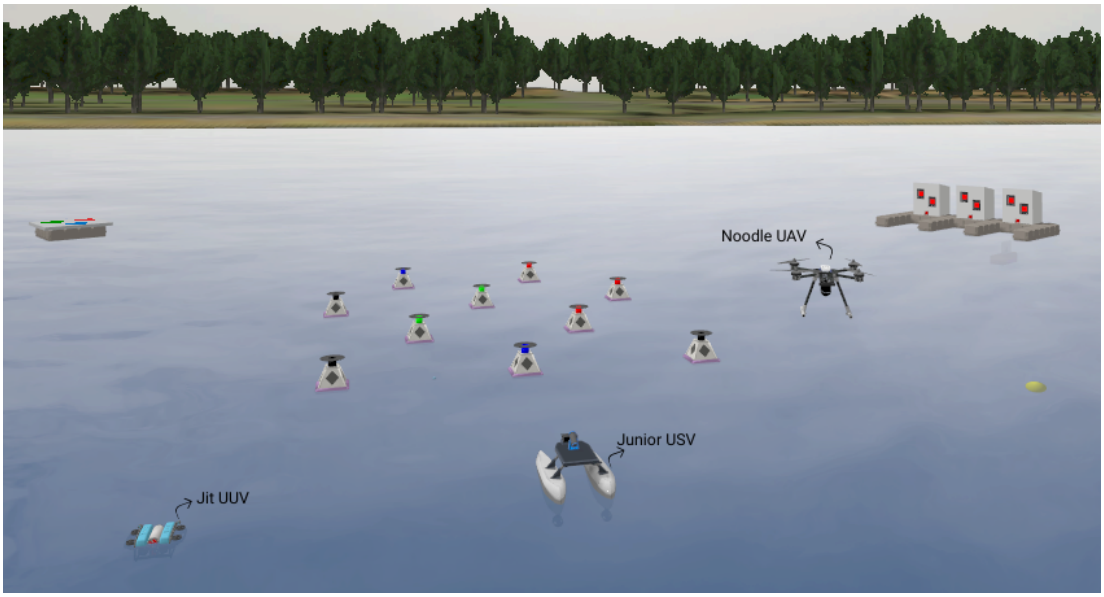


Fig. 12: RobotX 2026 course and simulated vehicles built by Team Minion in Gazebo using Virtual RobotX Tools [6]

promised to build up to autonomous on-water testing through a series of tests:

- In cage manual test.
- In cage autonomous test.
- On-water manual test.
- On-water autonomous test.

In the event of a failure at any stage, the UAV was required to restart from step 1 and successfully complete all prior steps before proceeding.

V. Competition Strategy

To design a competition strategy around new systems and tasks, Team Minion decomposed each task into the functions each UxV needed to complete the task. In the event multiple systems could provide the capability, Team Minion assigned the capability to the system with the most test time (USV over UAV or UUV, UAV over UUV). These capabilities are assessed at each task level (core, advanced, and disruptive) given each may change or add objectives. The result of this task decomposition is given in Table I.

From task decomposition, each task capability is given a confidence score that denotes the team's confidence in Junior, JIT, or Kevin to perform as expected. These confidences are scored on a 0% to 100% scale, as shown in Table II, with scores reviewed by members of each team (USV, UAV, and UUV) and team advisors for consensus and based on generalized performance in simulation and testing rather than task-specific performance. However, these confidence values may change due to favorable or unfavorable environmental factors, such as wind, ambient lighting, and current or future testing results.

Statistically, this provides a mechanism to assess the confidence in the team's ability to perform any task by applying the rules of probability. For instance, if two functions are required to complete a task, this results in statistical dependence where probabilities are multiplied as given by:

$$C_i = \prod_{j=1}^{n} c_j \tag{1}$$

where c_j is the confidence in tool j, as described in Table II, resulting in task confidence C_i. As only the relative confidence of one task over another is important, confidences are then normalized by the maximum confidence among all the tasks for easier comparison, resulting in:

$$NC_i = \frac{C_i}{\max C_k} \tag{2}$$

where the normalized task confidence is given by NC_i. The normalized confidences for each task that results from this analysis is given in Table III. This process allows for mathematical assessment of relative likelihood of success rather than

TABLE I: Task required capabilities

Task required capabilities				
Task	**Category**	**USV FNC**	**UAV FNC**	**UUV FNC**
Safe Passage	Core	Obj Identification Path Following		
	Advanced		Auto Navigate Obj Identification	
	Disruptive			
Infrastructure Repair	Core	Obj Identification		Waypoint Follow Obj Identification
	Advanced		Deliver Payload	Probe Placement
	Disruptive		Retrieve Payload	
Coordinated Logistics	Core	Dock Detection Water Delivery		
	Advanced		Deliver Payload Retrieve Payload Obj Identification	
	Disruptive			
Dynamic Response	Core	Waypoint Follow	Waypoint Follow	
	Advanced	Geo Fence	Geo Fence	
	Disruptive	Re-Planning	Re-Planning	

TABLE II: Confidence level in Minion's toolset (0 = no confidence, 100 = perfect confidence).

Tool	Confidence (0–100)
USV Tools	
Path Following	95
Obj Identification	95
Dock Detection	95
Water Delivery	20
Geo Fence	80
Re-planning	5
UAV Tools	
Auto Navigate	70
Object Identification	25
Retrieve Payload	50
Deliver Payload	60
Geo Fence	95
Re-Planning	5
UUV Tools	
Waypoint Follow	75
Underwater Identification	5
Probe Placement	5

purely subjective decision-making. The last column of Table III ranks tasks by normalized confidence, which provides a priority list for testing at competition and executing during a scored run. This approach has the additional benefit of being adaptable at competition where additional testing may change the confidence of any of the capabilities in Table II. Similarly, once scoring is released by RoboNation, the confidences can be multiplied by point totals to re-rank based on expected point value instead of confidence alone.

TABLE III: Task Confidence

Task Confidence			
Task	**Category**	**Normalized**	**Rank**
Safe Passage	Core	0.999	1st
	Advanced	0.700	3rd
	Disruptive	0.700	3rd
Infrastructure Repair	Core	0.039	9th
	Advanced	0.001	10th
	Disruptive	0.001	10th
Coordinated Logistics	Core	0.211	6th
	Advanced	0.063	7th
	Disruptive	0.063	7th
Dynamic Response	Core	0.737	2nd
	Advanced	0.560	5th
	Disruptive	0.001	10th

The analysis of Table III shows that the highest confidence is placed in the core capability of the safe passage task, with the second most confident task being the core capabilities of the dynamic response task. It should also be noted that confidence scores drop by a factor of three between the 6th and 7th ranked task levels. As such, these top six are currently considered the most likely tasks to be attempted by Team Minion at competition. However, MinionTask executes tasks in the predefined order given by the rankings of Table III. Recall that each task is written as a modular process (i.e. a ROS node) that requires identification of a minimum set of task cues in order to initiate. The task manager combines the task priority list and the list of tasks that are available in order to execute the highest priority task that is available for execution.

ACKNOWLEDGMENTS

Team Minion would like to thank our generous external partners for their support over the last three years: JAVAD (GNSS equipment donation), Volz (Servo Donation), RoboNation (grant support), Gene Haas Foundation (financial support), WaterLinked (educational discount), Blue Robotics (educational discounts), and DS Solidworks (software license donation). Team Minion would also like to thank their internal partners: the Embry-Riddle Aeronautical University College of Engineering, Mechanical Engineering Department, Unreel Media (Video Production), and Student Government Association (Embry-Riddle) for their financial support.

Many individuals have contributed significantly to the success of team Minion, but the team would like to give a special recognition to our wonderful alumni, who continue to support the team through technical assistance. The team would also like to thank Bill Russo, Travis Billette and Mike Potash for their fabrication assistance, and Christina Groenenboom, Brenda Carr, and Lisa Petko for logistics support.

REFERENCES

[1] Project Management Institute. (2017). Agile practice guide. Project Management Institute.

[2] K. Schwaber and J. Sutherland. (1991) The Scrum Guide The Definitive Guide to Scrum: The Rules of the Game. [Online]. Available: www.scrum.org

[3] Team Minion, "Design of the Minion research platform for the 2018 Maritime RobotX Challenge," Embry-Riddle Aeronautical University, Daytona Beach, FL, USA, Tech. Rep., 2018. [Online]. Available: https://robonation.org/app/uploads/sites/2/2019/09/ERAU_RX18_Paper.pdf. Accessed: Sept. 17, 2026.

[4] RSS, "RobotX Team Handbook." [Online]. Available: https://robonation.gitbook.io/robotx-2026-team-handbook. Accessed: Aug. 23, 2026.

[5] Coyle, E. J. 2025. " Efficient Grid-Based Clustering and Concave Hull Extraction for Unstructured Point Clouds." Journal of Field Robotics 43: 1925–1939. https://doi.org/10.1002/rob.70134.

[6] Toward Maritime Robotic Simulation in Gazebo, Brian Bingham and Carlos Aguero and Michael McCarrin and Joseph Klamo and Joshua Malia and Kevin Allen and Tyler Lum and Marshall Rawson and Rumman Waqar, Proceedings of MTS/IEEE OCEANS Conference, 2019, Seattle, WA, October

[7] Schoener, M.; Coyle, E.; Thompson, D. An anytime Visibility–Voronoi graph-search algorithm for generating robust and feasible unmanned surface vehicle paths. Auton. Robot. 2022, 46, 911–927, https://doi.org/10.1007/s10514-022-10056-7.

[8] Canadian Space Agency, "About Canadarm2," Latching End Effector description. Available: https://www.asc-csa.gc.ca/eng/iss/canadarm2/about.asp

[9] "Technical Design Report Team Minion RoboBoat 2026". Available: https://robonation.org/app/uploads/sites/3/2026/02/TDR_TeamMinion_RB2026.pdf

[10] Coyle, E.; White, D.; Currier, P. "Navigation and Control for Autonomous Vessels," U.S. Patent Application 456.023US1 July 2024.

Appendix A: Test Plan for the Team Minion Multi-Domain Fleet

Team Minion

Team Minion tests its vehicles in four stages: computer-aided analysis, bench testing, platform integration, and field testing. This appendix covers the integration and field stages for Junior (USV), JIT (UUV), Noodle (UAV), and one flight test of Kevin (UAV), which was not selected for competition. Each test states its environment and pass criteria. A test passes after one successful run, because the team tests regularly. Of 16 planned tests, 14 are complete and 2 are in progress.

The proof of readiness (POR) submission deadline was August 31. The final deadline, including all revisions, is October 12. The competition runs November 8–14.

A. Test Environments and Procedures

1) Environments: Bench and integration tests were run in the ERAU Robotics Lab. Water tests for the USV and UUV were run at the ERAU Pool, which measures $10\,\mathrm{ft}$ by $50\,\mathrm{ft}$ with a depth from $3\,\mathrm{ft}$ to $15\,\mathrm{ft}$. UAV tests were run in the ERAU Drone Cage, a netted enclosure measuring $50\,\mathrm{ft}$ by $50\,\mathrm{ft}$ by $30\,\mathrm{ft}$.

2) Personnel and safety: USV and UUV water tests require an RC driver, a dock hand, and a ground-station operator. Physical and RC emergency stops are verified before every test. For autonomous runs, the RC driver is always ready to take over. UAV testing follows a staged sequence: in-cage manual, in-cage autonomous, on-water manual, and on-water autonomous. After a failure at any stage, the UAV restarts from the first stage.

3) Data collection: ROS bag files capture all sensor data and inter-algorithm communication during tests. The bags are stored on the team network-attached storage. After each test, the team holds a debrief covering results, issues, and tasks for the next test.

B. USV (Junior) Test Plan

1) System under test: Junior is a quarter-scale USV that serves as the mothership of the fleet. It uses rigid foam pontoons and omni-directional control from two yaw-actuated Blue Robotics T200 thruster pairs. Perception uses three Livox Horizon LiDARs and an HDR camera. Localization uses a JAVAD DELTA-DI GNSS/IMU. Compute is a MINISFORUM MS-01 running ROS 2.

2) Test summary: Table I lists the USV tests and their pass criteria.

3) Proof of readiness criteria (USV-007): **Autonomous navigation video:** in a fully autonomous run, the USV starts $3\,\mathrm{m}$ behind the gate and passes through both sets of gates. The USV must not strike any buoys and must demonstrate good autonomous control throughout the run.

Safety systems, file upload: drawings of the kill switch wiring, photos of clearly marked tow points with a proper tow harness, photos of clearly marked lift points and lift harness, photos of propeller shrouds, and a functional block diagram with photos of the R/C approach showing operation independent of a laptop connection.

Safety systems, video: the onboard and remote kill switches operating correctly, and the visual feedback system operating in auto, manual, and kill states.

C. UUV (JIT) Test Plan

1) System under test: JIT is a bimodal UUV built on a Blue Robotics BlueROV2 Heavy and operated inverted for roll stability. A periscope carries a $5\,\mathrm{GHz}$ Ubiquiti Bullet, a $2.4\,\mathrm{GHz}$ RC link, and a GNSS receiver, so JIT runs untethered on the surface. A Water Linked A50 Doppler Velocity Log (DVL) provides submerged localization. Perception uses a Ping360 scanning sonar, an Omniscan FS450 side-scan sonar, and a low-light HD USB camera. Low-level control runs ArduSub on a BlueROV Navigator board with BlueOS on a Raspberry Pi 4B. A second Raspberry Pi 4B running Ubuntu 22.04 and ROS 2 Humble acts as the companion computer and connects through MAVROS. A normally-open relay cuts thruster power on an e-stop button, wireless, or lost-communication trigger, and JIT is positively buoyant, so it floats to the surface.

2) Test summary: Table II lists the UUV tests and their pass criteria. The waypoint tolerance of $\pm 50\,\mathrm{cm}$ used in UUV-002 to UUV-004 is stricter than the $\pm 1\,\mathrm{m}$ design goal for JIT.

3) Proof of readiness criteria (UUV-005): **Autonomous demonstration video:** in a fully autonomous run, the UUV starts $3\,\mathrm{m}$ behind the gate, submerges, passes through the gate, circles the marker, and passes back through the gate. Everything attached to the UUV must submerge with the vehicle. The UUV must not breach the surface, must not strike any buoys, and must demonstrate good autonomous control throughout the run. The video must make it clear that the vehicle maneuvered around the marker.

Course: a horizontal gate $2\,\mathrm{m}$ wide and positioned $1\,\mathrm{m}$ below the water surface, and a vertical marker positioned $10\,\mathrm{m}$ beyond the gate.

Safety systems, file upload: drawings of the kill switch wiring, photos of clearly marked tow points with a proper tow harness, photos of clearly marked lift points and lift harness, photos of propeller shrouds, a photo of the mounting area for the locator beacon, and a functional block diagram with photos of the R/C approach showing operation independent of a laptop connection.

Safety systems, video: the onboard kill switch operating correctly, the visual feedback system operating in auto, manual, and kill states, and proof that the system is positively buoyant.

TABLE I: USV Test Summary

ID	Test	Environment	Pass Criteria	Date	Status
USV-001	Pontoon assembly	Robotics Lab	Deck trim 1–2°	Jul 10	Complete
USV-002	Pontoon water test	ERAU Pool	Trim 1–2°; draft 40–50 %; no water ingress	Jul 11	Complete
USV-003	GPS calibration	Robotics Lab	$\leq$30 cm position error and $\leq$1° heading error against a surveyed reference	Aug 15	Complete
USV-004	GPS time sync	Robotics Lab	$\leq$2 ms clock offset using IEEE 1588 v2 PTP	Aug 16	Complete
USV-005	Lidar calibration	Robotics Lab	$\leq$2 cm inter-lidar object position disagreement (CAD extrinsics refined with ICP); $\leq$2 ms time sync	Aug 25	Complete
USV-006	Controls testing	ERAU Pool	Surge, sway, and yaw error within $\pm$20 cm and $\pm$3°	Aug 26	Complete
USV-007	Proof of readiness	ERAU Pool	Handbook POR criteria met (§3)	Aug 28	Complete
USV-008	Path following	ERAU Pool	$\leq$10 cm cross-track error	Sep 4	In progress

TABLE II: UUV Test Summary

ID	Test	Environment	Pass Criteria	Date	Status
UUV-001	Manual controls test	ERAU Pool	Each e-stop trigger (button, wireless, lost communication) cuts thruster power; JIT surfaces on its own after each trigger; RC manual control of surge, sway, heave, and yaw works	Sep 4	Complete
UUV-002	Sensors and auto controls test	ERAU Pool	IMU, depth, GPS (surface), and DVL publish valid data; autonomous waypoint reached within $\pm$50 cm	Sep 16	Complete
UUV-003	Surface waypoints test	ERAU Pool	Start at an entry gate, go straight, circle an object, and return through the gate within $\pm$50 cm	Sep 17	Complete
UUV-004	Submerged waypoints test	ERAU Pool	Same pattern as UUV-003, submerged using DVL dead reckoning, within $\pm$50 cm	Sep 20	Complete
UUV-005	Proof of readiness attempt	ERAU Pool	Handbook POR criteria met (§3); only the visual feedback indicator remains	Sep 30 (target)	In progress

D. UAV Test Plan

1) System under test: Noodle is the competition UAV. It uses a Tarot Iron Man 650 carbon fiber frame and a CUAV Pixhawk V6X V2 flight controller running PX4. Localization uses a Neo 3 GPS antenna with the Pixhawk built-in GPS receiver and IMU. Perception uses an e-CAM86 CUONX camera with a 110° field of view, and Noodle carries no LiDAR. A Jetson companion computer and a Ubiquiti Bullet handle processing and communication. Propulsion is four T-Motor U5 400kV brushless motors with T-Motor ALPHA 40A ESCs and 16×5.4 propellers, powered by two Auline S70 Li-ion batteries in a 6S2P configuration. Measured flight time is about 35 min.

Kevin is a heavy-lift UAV with a capture mechanism (see the UAV Tin Capture Mechanism appendix). It was not selected for competition because of its many modifications, and only its manual flight stability test is recorded here.

2) Test summary: Table IV lists the UAV tests and their pass criteria.

3) Proof of readiness criteria (UAV-002): **Flight demonstration video:** an introduction that identifies the school and team, a description of safety risks and mitigations, and flights in manual and autonomous operation. Each flight shows proof of the operating mode, takeoff to above 3 m AGL, the handbook flight pattern, proof that the UAV stays within the published geofence and below the maximum altitude even when commanded to exceed them, and a landing. The flight patterns are defined in the UAV Flight Patterns section of the RobotX 2026 team handbook.

Safety systems, file upload: photos of the mounting area for the emergency recovery light, photos of clearly marked safe handling areas for recovery, and documentation of UAV behavior on loss of link with the remote controller, low battery, task or mission abort, and geofence boundary reached.

Safety systems, video: proper operation on loss of link with the remote controller, compliance with geofence boundaries, and proof that the system is positively buoyant.

Remote controller compliance: documentation of the remote controller approach and an image or video of the dedicated remote controller.

E. Key Dates

Table III lists the deadlines that govern the open tests.

TABLE III: Key Dates (2026)

Date	Event
Aug 31	POR submission deadline
Sep 30	Target completion of UUV-005
Oct 12	Final deadline with all revisions
Nov 8–14	RobotX competition

TABLE IV: UAV Test Summary

ID	Test	Environment	Pass Criteria	Date	Status
UAV-001	Manual and auto flight test (Noodle)	Drone Cage	Stable manual and autonomous flight; RC kill and failsafe function; geofence compliance; autonomous waypoint completion	Aug 20	Complete
UAV-002	UAV proof of readiness (Noodle)	Drone Cage	Handbook POR criteria met (§3)	Aug 25	Complete
UAV-003	Manual flight stability test (Kevin)	Drone Cage	Takes off and flies in manual mode. Passed; tuning was needed for smooth flight. Kevin is not selected for competition	Sep 18	Complete

Appendix B: Design and Analysis for the UAV Tin Capture Mechanism

Sarthak Aggarwal, Mateus Prudencio

F. Purpose and Rule Context

Under the RobotX 2026 Team Handbook, Section 3.3, Mission Tasks 2 and 3 require the UAV to autonomously *locate, retrieve, and deliver* one of three colored resource "tins" between floating platforms [1], [2]. At the Advanced Tier, the UAV may deliver *any* tin; at the Disruptive Tier, it must identify and retrieve the *correct* tin (RED, GREEN, or BLUE) based on a relayed two-color light sequence, then place it inside the matching 60–70 cm diameter circle on the delivery platform. The rulebook specifies the resource tins as aluminum cans, coated in spray Plasti-Dip for watertightness, with a target mass of **40–50** g [1]. This appendix documents the design, actuation, and load analysis of the capture mechanism carried by Kevin to satisfy this requirement without a conventional powered gripper, motorized claw, or vacuum system, instead using a passive-closing, string-capstan mechanism directly inspired from the CanadaArm2 Latching End Effector (LEE) design [4].

Tin geometry:

$$D_{\text{tin}} = 2.5\,\text{in} = 63.5\,\text{mm}, \qquad H_{\text{tin}} = 1.0\,\text{in} = 25.4\,\text{mm},$$

G. Mechanism Overview

The mechanism (Fig. 1) consists of four rigid wooden dowel arms pinned to a rotary hub at the base of the UAV frame. A single 24 V brushed DC gear-motor with an internal worm-gear reduction drives all four arms in synchronized rotation through an external $120:8$-tooth spur gear stage $(15:1)$. The free end of each dowel is connected by a length of **1/8-inch (3.2 mm) thick, textured TPU strap** to a fixed anchor on its adjacent landing gear leg.

In the open (stowed) position, each strap runs a short, direct, low-tension path from dowel tip to leg anchor, clear of the tin (Fig. 2). As the hub rotates the dowels inward through $\Delta\theta \approx 180^\circ$ (Fig. 1b), the tin blocks each strap's straight-line path and forces it to deflect around the tin's near side (Fig. 3). The resulting increase in path length stretches the TPU elastically, and that induced tension – amplified by capstan friction over the wrap contact – produces a net inward, self-centering grip from all four straps. Unlike a shrinking-circumference noose or purse-string, no strap is fed or taken up by the drivetrain: each is a fixed-length elastic tether whose grip comes from being forced to detour around the tin, not from cordage being winched.

The design is a structural analog of the NASA/CSA **Latching End Effector (LEE)** on the Space Station Remote Manipulator System (Canadarm2), which uses three motor-driven snare cables tightening radially around a grapple fixture to achieve a self-centering, over-constrained grip [3], [4]. Kevin's mechanism applies the same principle – self-centering closure from multiple independently-actuated tethers – with four elastically-deflected TPU straps in place of winched snare cables, and a worm-gear DC motor in place of the LEE's ball-screw drive. The worm reduction is self-locking (§5), so the closed state holds with the motor de-energized, eliminating continuous power draw during flight with a loaded tin – similar to the passive-retention strategies documented for compliant aerial grippers in Fantoni *et al.* [5].

H. Kinematics of Dowel Closure

Each strap's end-to-end path length grows from L_{open} (open, taut, unstressed) to L_{closed} (closed, deflected around the tin) as the dowel sweeps through $\Delta\theta$. No length is fed in by the drivetrain – the same fixed-length strap simply stretches to accommodate the longer wrapped path, and this induced elastic tension is what generates the capstan grip (§I).

$$\begin{aligned} L_{\text{open}} &\approx 210\,\text{mm}, & L_{\text{closed}} &\approx 300\,\text{mm}, \\ r_a &= 141\,\text{mm}, & \Delta\theta &= 180^\circ, \end{aligned} \tag{1}$$

where r_a is the dowel's pivot-to-strap-anchor radius and $\Delta\theta$ is the hub sweep from open to fully-crossed. L_{closed} is consistent with the strap wrapping roughly half the tin's circumference ($\pi D_{\text{tin}} \approx 200\,\text{mm}$) plus the two straight segments connecting the wrap to the dowel tip and leg anchor.

1) Elastic strain: Because $L_{\text{closed}} > L_{\text{open}}$ and the strap's physical length is fixed, closure imposes a uniaxial elastic strain of

$$\varepsilon = \frac{L_{\text{closed}} - L_{\text{open}}}{L_{\text{open}}} = \frac{300 - 210}{210} \approx 0.429 \approx \mathbf{42.9\%}. \tag{2}$$

TPU elastomer typically exhibits elongation-at-break of **300%–800%** [8], so a $\sim$43% operating strain carries roughly an order of magnitude of margin below rupture – comfortably within the material's elastic range for a low-cycle-count application. The strap is treated as a reusable elastic element across many capture/release cycles; §L tracks fatigue/creep as a wear item.

2) From strain to strap tension: The elastic tension induced in each strap by this forced elongation is, to first order (treating the TPU as linear-elastic over this strain range, a simplification discussed further in §K),

$$T_{\text{elastic}} = k_{\text{strap}}\,\varepsilon\,L_{\text{open}}, \tag{3}$$

where k_{strap} is the strap's effective axial stiffness (force per unit strain per unit length), a property of the TPU tape's cross-section and material modulus. This tension T_{elastic} is the T_{hold} term that feeds the capstan relation of §I: **the grip force in this design comes from strap elasticity, not motor-maintained winch tension**. Once the dowel is driven closed and held there by worm-gear self-locking (§5), the strap tension – and therefore the tin's grip – persists indefinitely with zero motor holding torque, since the strain is geometrically locked in by



(a) Isometric render of the capture mechanism, stowed tin (blue) shown for scale.



(b) Top (plan) view showing the crossed dowel-arm pairs and central drive hub.



(c) Side view of the closed (crossed) dowel arms beneath the landing legs.

Fig. 1: Kevin's four-dowel tin capture mechanism, CAD renders.

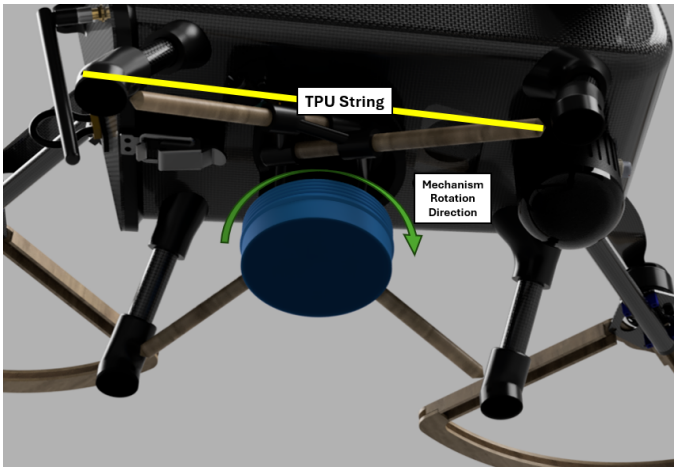


Fig. 2: Open (stowed) position: each TPU strap runs a short, direct, low-tension path from its dowel tip to the anchor point on the adjacent landing gear leg, clear of the tin.

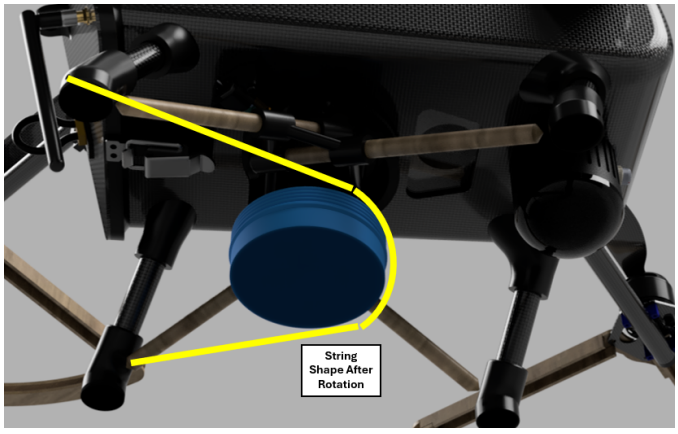


Fig. 3: Closed position, after $\Delta\theta \approx 180^\circ$ of dowel rotation: the tin now obstructs the strap's straight-line path, forcing it to deflect around the tin's near side. The resulting increase in path length ($L_{\text{open}} \rightarrow L_{\text{closed}}$) elastically stretches the TPU strap, and the induced tension combined with the wrap angle produces the capstan grip.

the dowel position. The motor's job during closure is instead to rotate the dowel through $\Delta\theta$ against the strap's growing elastic resistance, with required torque rising through the stroke as T_{elastic} increases.

At $\varepsilon = 42.9\%$, $T_{\text{elastic}} \approx 8\,\text{N}$: the strap is easy to stretch by hand through most of its range but resists strongly near full

extension, typical of TPU's strain-hardening curve. This value is consistent with bench observation – the mechanism closes reliably, with the motor drawing toward stall current and little torque margin to spare (§K) – and is used throughout §I–§**??**. Equivalent strap stiffness: $k_{\text{strap}} \approx 89\,\text{N}$ (Eq. (3)).

I. Capstan Friction Model of the Strap–Tin Interface

The retention force holding the tin against gravity, aerodynamic disturbance, and flight-load accelerations is generated entirely by **capstan (belt-friction) action**: the TPU strap wraps the tin through an angle ϕ and the friction between strap and tin (aided by the tin's Plasti-Dip elastomeric coating) converts tension differential across the wrap into a hold force normal to the tin surface. The governing relation is the classical Euler–Eytelwein capstan equation:

$$\boxed{T_{\text{load}} = T_{\text{hold}}\, e^{\mu\phi}} \tag{4}$$

where T_{hold} is the strap tension on the anchor side of the wrap, T_{load} is the maximum tension the strap can resist on the tin-retention side before slip, μ is the strap-on-Plasti-Dip friction coefficient, and ϕ is the wrap angle in radians. Each strap contacts the tin over $\phi \approx \pi$ ($\approx 180°$) once closed (Figs. 2–3) – enough to capture most of the capstan equation's exponential amplification (Table I), the same principle that lets a sailor hold tons of line tension on a winch capstan with a few kilograms of hand force. Here $T_{\text{hold}} = T_{\text{elastic}}$ (Eq. (3)): the tension comes from forced strap elongation, not a motor-driven pulley.

At $H_{\text{tin}} = 25.4\,\text{mm}$, the $3.2\,\text{mm}$ strap occupies about 13% of the tin's height per wrap – narrow enough to sit as a clean band clear of the rim and base radius.

1) Friction coefficient: TPU-on-TPU and TPU-on-soft-polymer interfaces typically exhibit $\mu \approx 0.5$–0.9 [7]. We use $\mu = 0.5$ (conservative) for capacity sizing and $\mu = 0.8$ (best case) to bound achievable performance, reflecting the textured strap surface against the Plasti-Dip coating.

2) Capstan amplification factor: At the confirmed $\phi = \pi$ (each strap's $180°$ contact):

$$e^{\mu\phi}\Big|_{\mu=0.5} = e^{0.5\pi} \approx 4.81,$$
$$e^{\mu\phi}\Big|_{\mu=0.8} = e^{0.8\pi} \approx 12.3.$$

TABLE I: Capstan amplification factor $e^{\mu\phi}$ for candidate wrap angles and friction coefficients.

Wrap angle ϕ	ϕ [rad]	$e^{\mu\phi}$ ($\mu = 0.5$)	$e^{\mu\phi}$ ($\mu = 0.8$)
$180°$ (single loop)	3.14	4.81	12.3
$216°$	3.77	6.59	19.4
$270°$	4.71	9.36	34.8
$360°$ (full overwrap)	6.28	23.1	151.5

The practical implication (Table I) is that even a modest capstan wrap (180–220°) provides a **5–20**× amplification between the low-tension side of each strap's wrap contact and the tension it can resist on the tin-retention side before slip. This is the central design justification for a strap-deflection capture mechanism rather than a direct pinch/clamp gripper: only a modest elastic strap tension (§H) is needed to generate a much larger effective retention force at the tin, and — because the motor's job is to stretch the strap into position rather than to directly react the full retention load at a jaw — the drivetrain torque requirement is correspondingly reduced (§K).

J. Static Retention Force Requirement

The retention force must react the tin's weight plus dynamic (flight) load factors. With tin mass $m_{\text{tin}} = 50\,\text{g}$ (rulebook upper bound, taken conservatively) [1]:

$$W_{\text{tin}} = m_{\text{tin}}\, g = (0.050\ \text{kg})(9.81\ \text{m/s}^2) = 0.4905\,\text{N}. \tag{5}$$

During aggressive maneuvering (acceleration, gust rejection, or a hard landing bump before the mechanism fully seats) the effective load can be modeled with a dynamic load factor n:

$$F_{\text{req}} = n \cdot W_{\text{tin}}. \tag{6}$$

Taking a conservative $n = 4$ (consistent with typical small-UAS shock/vibration design practice for externally carried payloads under gust and touchdown transients):

$$F_{\text{req}} = 4 \times 0.4905\,\text{N} \approx 1.96\,\text{N} \approx 200\ \text{gf}.$$

This is the minimum normal/retention force the strap system must sustain – trivially small given the payload's own 40–$50\,\text{g}$ mass. The mechanism is never friction- or strength-limited at the tin interface; the governing constraints are motor torque margin during closure (§K) and getting the wrap fully seated around an off-center or tilted tin.

K. Drivetrain Torque Budget

1) Motor and gearbox specification: The actuator is an NFP-GM1218-TB050S 15 mm micro DC worm-gear motor (Precision Mini Drives) [6], operated at the **12 V, internal ratio** $i_{\text{gb}} = 79:1$ configuration, per the datasheet (Table II):

TABLE II: NFP-GM1218-TB050S motor and gearbox datasheet ratings at 12 V.

	No-load	Rated load	Stall
Speed [rpm]	203	177	—
Current [mA]	55	300	1000
Output torque [gf·cm]	0	284	948

Converting the rated-load torque to SI units ($1\ \text{gf}\cdot\text{cm} = 9.806\,65 \times 10^{-5}\,\text{N m}$):

$$\begin{aligned}\tau_{\text{gearbox,rated}} &= 284\ \text{gf·cm} \times 9.80665 \times 10^{-5}\ \text{Nm}/(\text{gf}\cdot\text{cm}) \\ &= 0.027\,85\,\text{N m}, \end{aligned} \tag{7}$$

$$\begin{aligned}\tau_{\text{gearbox,stall}} &= 948\ \text{gf·cm} \times 9.80665 \times 10^{-5}\ \text{Nm}/(\text{gf}\cdot\text{cm}) \\ &= 0.092\,96\,\text{N m}. \end{aligned} \tag{8}$$

2) External gear reduction and total system ratio: **Note:** the $79:1$ ratio above is *internal* to the worm gearbox itself. The system uses an *additional external* spur gear pair between the gearbox output shaft and the dowel hub: a 120-tooth gear fixed to the dowel-carrying hub, driven by an 8-tooth pinion on the gearbox output shaft, giving

$$i_{\text{ext}} = \frac{N_{\text{hub gear}}}{N_{\text{pinion}}} = \frac{120}{8} = 15{:}1. \tag{9}$$

These two reductions are in series, so the total mechanical advantage from motor rotor to hub is

$$i_{\text{total}} = i_{\text{gb}} \times i_{\text{ext}} = 79 \times 15 = 1185{:}1. \tag{10}$$

Applying the external stage (assumed efficiency $\eta_{\text{ext}} = 0.90$ for a small open spur pair; a well-cut pair typically achieves 0.95–0.98, so this is conservative):

$$\begin{aligned}\tau_{\text{hub,rated}} &= \tau_{\text{gearbox,rated}} \times i_{\text{ext}} \times \eta_{\text{ext}} \\ &= (0.02785)(15)(0.90) = 0.376\,\text{N m}, \end{aligned} \tag{11}$$

$$\begin{aligned}\tau_{\text{hub,stall}} &= \tau_{\text{gearbox,stall}} \times i_{\text{ext}} \times \eta_{\text{ext}} \\ &= (0.09296)(15)(0.90) = 1.254\,\text{N m}. \end{aligned} \tag{12}$$

Correspondingly, output hub speed at rated load is reduced by the external stage:

$$n_{\text{hub}} = \frac{n_{\text{gb,rated}}}{i_{\text{ext}}} = \frac{177\ \text{rpm}}{15} = 11.8\,\text{rpm} \ \Rightarrow\ \omega_{\text{hub}} = 1.24\,\text{rad/s}. \tag{13}$$

3) Motor torque vs. strap elastic resistance: Unlike a winch-type mechanism, the drivetrain here does not directly set the strap tension by paying out or reeling in cordage; instead, it must supply enough torque, throughout the closing stroke, to rotate the dowel against the strap's growing elastic resistance as it is stretched from L_{open} to L_{closed} (§H). At any point in the stroke, the reaction torque the strap exerts back on the dowel is

$$\tau_{\text{strap}}(\theta) = T_{\text{elastic}}(\theta)\, r_a \sin\beta(\theta), \tag{14}$$

where $T_{\text{elastic}}(\theta)$ is the instantaneous strap tension from Eq. (3) and $\beta(\theta)$ is the local strap-to-dowel angle. This reaction torque peaks near the end of the stroke, where strain and wrap geometry are both largest. With $r_a = 141\,\text{mm}$, the maximum force the drivetrain can statically react at the strap anchor is

$$F_{\text{avail,rated}} = \frac{\tau_{\text{hub,rated}}}{r_a} = \frac{0.376\ \text{N·m}}{0.141\ \text{m}} \approx 2.67\,\text{N}, \tag{15}$$

$$F_{\text{avail,stall}} = \frac{\tau_{\text{hub,stall}}}{r_a} = \frac{1.254\ \text{N·m}}{0.141\ \text{m}} \approx 8.89\,\text{N}. \tag{16}$$

At $T_{\text{elastic}} \approx 8\,\text{N}$:

$$\frac{F_{\text{avail,rated}}}{T_{\text{elastic}}} \approx 0.33, \qquad \frac{F_{\text{avail,stall}}}{T_{\text{elastic}}} \approx 1.11. \tag{17}$$

Rated (continuous) torque alone does not close the mechanism – it falls short by $3\times$. Stall torque covers it, but with only $\sim$11% margin, consistent with bench operation: the mechanism closes reliably, with the motor drawing toward stall current on every cycle. This is exactly what the DRV8871's I_{TRIP} current limit (§**??**) is sized to tolerate without thermal damage. **This closing-torque margin, not the holding margin below, is the tighter constraint on this design.**

4) Retention capacity once closed: Once closed and held by worm-gear self-locking (§5), the strap tension available to resist the tin pulling free is the capstan-amplified elastic tension at full closure:

$$T_{\text{load,available}} = T_{\text{elastic}} \cdot e^{\mu\phi} \approx (8\ \text{N})(4.81) \approx 38.5\,\text{N}, \tag{18}$$

using $\mu = 0.5$, $\phi = 180^\circ$ ($e^{\mu\phi} = 4.81$, Table I). Against $F_{\text{req}} \approx 1.96\,\text{N}$ (Eq. (6)):

$$\text{Safety factor} \approx \frac{38.5\ \text{N}}{1.96\ \text{N}} \approx \mathbf{19.6}\times. \tag{19}$$

This holding margin is available with **zero motor current**: the strap's stretch is geometrically locked in by dowel position, not sustained by applied torque. The asymmetry with the tight closing margin above is a direct consequence of capstan amplification acting on the *holding* side of the load path but not on the *closing* side, where the motor reacts the bare strap tension directly.

5) Worm-gear self-locking: A worm gearbox is self-locking (back-driving-resistant) when the worm's lead angle λ satisfies

$$\tan\lambda < \mu_w, \tag{20}$$

where μ_w is the coefficient of friction between the worm and worm-wheel flank surfaces (typically $\mu_w \approx 0.05$–0.10 for a lubricated steel/bronze or steel/POM pair). Standard worm gearboxes of this class (single or double-start worm, high reduction ratio) are designed with λ well below this threshold specifically to provide self-locking, which is why worm gearing was selected for this application in the first place: **once the dowels are driven to the closed (crossed) position, the tin's weight and any inertial/aerodynamic disturbance load cannot back-drive the motor**, so grip is retained with zero holding current. This directly reduces UAV electrical load during the delivery flight leg and removes a failure mode (motor stall/overheat while holding a payload against continuous load).

L. Failure Modes and Mitigations

TABLE III: Failure Mode and Effects summary for the tin capture mechanism.

Failure mode	Effect	Mitigation
Strap slip at low μ (wet/degraded Plasti-Dip)	Tin drops during transit; mission point loss	Capstan amplification $e^{\mu\phi} \approx 4.8$–$12.3\times$ (Table I); textured TPU increases real contact area vs. smooth cordage
Motor stall while closing on off-center tin	Incomplete capture, undetected by the MCU (no feedback from DRV8871, §**??**)	I_{TRIP} hardware backstop prevents thermal damage; fixed-duration closure timing with margin; vision-guided re-centering before closure
Worm gearbox failure or mechanical jam in closed state	Payload stuck; open-loop control can't distinguish this from normal closed-and-idle	Pre-flight functional test of release cycle; mechanical over-travel stop with manual release tab
Dowel arm bending/fatigue failure	Loss of geometric constraint, asymmetric grip	2.7–$4.5\times$ static safety factor (§**??**); periodic visual inspection for grain damage
Strap wear/abrasion over repeated cycles	Gradual μ degradation, reduced capstan margin	TPU chosen over natural-fiber cordage for abrasion resistance; strap replaceable as consumable
Partial wrap (tin not fully $180^\circ+$ enclosed)	Capstan amplification collapses toward linear regime, Table I	Kinematic margin (§H) sized for full-wrap closure despite tin positioning tolerance
No feedback path from DRV8871 driver (open-loop control only)	Ambiguous mechanism state; can't confirm closure, release, or distinguish stall from success	Bench-calibrated fixed-duration drive commands; hardware current-trip protects motor winding; indirect vision/mass-based confirmation at the vehicle level
Thin closing-stroke torque margin ($\sim$11% at stall, §K)	Sensitive to friction/voltage variation; a degraded motor, low battery, or added mechanical friction could stall the closing stroke before full wrap	DRV8871 I_{TRIP} tolerates sustained near-stall operation without damage; monitor battery voltage sag; fallback options if margin degrades further: softer strap, larger r_a, more gear reduction

M. Summary

The four-dowel strap-deflection mechanism retrieves and delivers a 40–$50\,\text{g}$ resource tin per RobotX 2026 Tasks 2 and 3 [1], [2], using a single $24\,\text{V}$ worm-gear motor and a $120:8$-tooth $(15:1)$ external reduction to drive four dowel arms. Each of four TPU straps runs taut and unstressed from a dowel tip to a landing-gear-leg anchor when open; as the dowel sweeps $\Delta\theta = 180^\circ$ ($r_a = 141\,\text{mm}$), the tin blocks each strap's path and forces it to deflect around the tin's near side, stretching it from $L_{\text{open}} \approx 210\,\text{mm}$ to $L_{\text{closed}} \approx 300\,\text{mm}$ ($\varepsilon \approx 42.9\%$ strain, well within TPU's 300–800% elongation-at-break [8]). The induced elastic tension, amplified by capstan friction at $\phi \approx 180^\circ$ (Eq. (4)), produces the grip – not a motor-maintained winch force. Worm-gear self-locking (Eq. (20)) holds the closed position with zero continuous power draw; the drivetrain's job is only to supply torque transiently during closure. Structural loads on the dowel arms carry a 2.7–$4.5\times$ safety factor. The design shares its self-centering, over-constrained, multi-tether closure principle with the Latching End Effector flown on Canadarm2/SSRMS [3], [4], substituting elastic strap deflection for winched snare cables. The mechanism is driven open-loop by a DRV8871 H-bridge with no position or current feedback to the flight controller and state is inferred from fixed-duration drive commands.

Key finding: at $T_{\text{elastic}} \approx 8\,\text{N}$ – consistent with bench operation, where the mechanism closes reliably but draws toward stall current – **closing-stroke torque margin, not holding margin, is the tighter constraint** on this design. Rated motor torque alone cannot close the mechanism; stall torque covers it with only $\sim$11% margin. Retention once closed is comfortable at $\sim 20\times$. The thin closing margin is the parameter to watch as the design matures – a weaker battery, colder motor, or added friction has the least room to absorb before affecting reliable closure.

REFERENCES

[1] RoboNation, "3.3.3 Mission Task 2: Infrastructure Survey and Repair," *RobotX 2026 Team Handbook*, Section 3: Autonomy Challenge. Available: https://robonation.gitbook.io/robotx-2026-team-handbook/section-3-autonomy-challenge/3.3-mission-task-descriptions/3.3.3-mission-task-2-infrastructure-survey-and-repair

[2] RoboNation, "3.3.4 Mission Task 3: Coordinated Logistics," *RobotX 2026 Team Handbook*, Section 3: Autonomy Challenge. Available: https://robonation.gitbook.io/robotx-2026-team-handbook/section-3-autonomy-challenge/3.3-mission-task-descriptions/3.3.4-mission-task-3-coordinated-logistics

[3] NASA, "Mobile Servicing System," NASA International Space Station Reference Guide. Available: https://www.nasa.gov/international-space-station/mobile-servicing-system/

[4] Canadian Space Agency, "About Canadarm2," Latching End Effector description. Available: https://www.asc-csa.gc.ca/eng/iss/canadarm2/about.asp

[5] G. Fantoni *et al.*, "Design and analysis of compliant end-effectors for lightweight aerial manipulation," *Mechanism and Machine Theory*, ScienceDirect, 2025. Available: https://www.sciencedirect.com/science/article/pii/S092442472500617X

[6] Precision Mini Drives, "15mm Micro DC Gear Motor – 44mm Type, Model NFP-GM1218-TB050S," product datasheet. Available: https://precisionminidrives.com/product/15mm-micro-dc-gear-motor-44mm-type-model-nfp-tb050-s

[7] Representative coefficient-of-friction ranges for thermoplastic polyurethane (TPU) against soft elastomeric/polymer coatings, standard engineering materials references (e.g. ASM Engineered Materials Handbook, polymer tribology tables).

[8] Representative elongation-at-break ranges for thermoplastic polyurethane (TPU) elastomer, typically 300–800 % depending on hardness/formulation, per standard engineering materials references (e.g. Xometry materials data, ASM Engineered Materials Handbook).

[9] Forest Products Laboratory, *Wood Handbook: Wood as an Engineering Material*, USDA Forest Service, General Technical Report FPL-GTR-282. Typical modulus of rupture (bending strength) values for common dowel hardwood species (birch, maple, ash).

[10] Texas Instruments, *DRV8871 3.6-A Brushed DC Motor Driver With Internal Current Sense (PWM Control)*, datasheet Rev. B. Available: https://www.ti.com/lit/ds/symlink/drv8871.pdf

[11] "DRV8871 Single Brushed DC Motor Driver: TI Chip Explained," Zbotic, current-limit resistor sizing reference ($I_{\text{limit}} = V_{\text{ILIM}}/R_{\text{ISEN}}$). Available: https://zbotic.in/drv8871-single-brushed-dc-motor-driver-ti-chip-explained/

[12] Adafruit Industries, *Adafruit DRV8871 Brushed DC Motor Driver Breakout*, product guide (reference design: 30 kΩ R_{ILIM} for ∼2 A default limit). Available: https://www.mouser.com/datasheet/2/737/adafruit_drv8871_brushed_dc_motor_driver_breakout-1396486.pdf

Appendix C: Jit: An Unmanned Underwater Maritime Robotics Platform

Sean Johnson, Joshua Wenger, Alexander Kilian

Unmanned Underwater Vehicle "Jit" — Maritime RobotX Challenge 2026. Proof-of-Readiness Autonomy Demonstration and Safety Requirements.

A. Introduction

The 2026 RobotX Competition will take place in Singapore from Nov 8–14, 2026. A challenge returning to the RobotX Competition is the inclusion of underwater autonomy completed by an Uncrewed Underwater Vehicle (UUV), after being absent since 2018. To that end, the ERAU RobotX team Minion has worked towards fielding a new UUV since the UUV used for RobotX 2018 is no longer operable [1]. The new UUV, hereafter referred to as "Jit" is built off of a Blue Robotics BlueROV2 Heavy platform. The prebuilt submarine has undergone significant modifications and testing to make it ready for the competition. This document details the modifications and design decisions made to satisfy the proof of readiness requirements set out by RoboNation [2].

B. Related Work

The RobotX Maritime Challenge previously included a dedicated UUV task in 2018, which will return for the 2026 competition. In 2018, four teams deployed UUVs: Team Minion, Team QUT, Team Owltonomous, and Team Bumblebee [1], [3], [4], [5]. Of these systems, only Team QUT's vehicle operated autonomously, although it remained tethered to the USV for telemetry, communication, and E-stop functionality. Two teams used prebuilt platforms, while the other two used custom-built vehicles. Team Minion operated a Blue Robotics BlueROV2 in its standard configuration, Team QUT used a RangerBot AUV, and Team Owltonomous adapted an existing vehicle previously developed for the RoboSub competition. Team Bumblebee deployed a custom-built vehicle designed specifically for the RobotX UUV task [5].

RoboSub, a related RoboNation competition, also requires teams to design and operate UUVs for a range of underwater tasks. Although pre-built platforms are permitted, the competition encourages original vehicle development, and all teams competing in 2025 used custom-built platforms [7]. A common challenge in these systems is maintaining reliable underwater localization without access to Global Navigation Satellite System (GNSS). A frequently used approach combines inertial measurements, magnetometer-based heading estimates, and DVL estimates of motion. Team BRACU Duburi and Team DAVE both used ArduPilot with DVL-based localization [8], [9]. Team BRACU Duburi additionally incorporated camera-based optical navigation. The benefits of optical navigation would not be worth the work required to implement it. Although optical navigation may be valuable for later competition tasks, it was not considered necessary for the proof-of-readiness demonstration described in this work.



Fig. 1: Blue Robotics BlueROV2 Heavy [6].

Other teams also addressed mechanical and thermal-management challenges relevant to Jit. Based on prior experience with its selected components, Team All Blue distributed its electronics across two aluminum enclosures to improve heat dissipation [10]. Because Team Minion identified its thermal-management limitations only after the major components had been selected, three internal fans were instead added to circulate air and transfer heat across the larger enclosure surface area.

Team DOB HydroJan similarly used ROV Maker components for its electronics enclosures and documented successful leak testing and deployment at comparable depths [11]. Team DOB HydroJan tested their ROV Maker parts and saw success in the deployment of those enclosures at depths seen in the RoboSub competition comparable to the depth of our proof of readiness course.

C. Requirements and Design Strategy

1) Proof of readiness requirements: The main objectives of the proof of readiness are safety and the autonomy demonstration. The autonomy demonstration is intended to show that each team has developed a platform to a state that it can autonomously maneuver through an environment and do so safely. The autonomy demonstration requirement dictates that the UUV must traverse through a submerged gate, circle around a marker buoy, and return to the same starting point through the submerged gate [2]. The vehicle must fully submerge, must not breach the surface during the run, and must not strike any buoys or other objects during the run. Fig. 2 provides an example of the proof of readiness course provided by RoboNation.

The remaining requirements are primarily concerned with safety of the vehicle and safety of the person(s) operating around the vehicle. Listed below are the safety requirements.

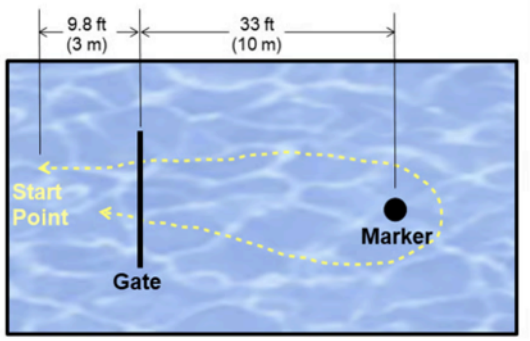


Fig. 2: Proof of readiness autonomy course [2].

A. A working Estop system that disconnects power from the motors or otherwise places the motors in a safe configuration along with a diagram.
B. Clearly marked tow points and lift points for moving and transporting the vehicle by external power.
C. A working remote control system that can pilot the vehicle as well as remotely activate the Estop system separate from a ground control computer along with diagrams.
D. Proof that the motors are protected so that the propellers pose minimal threat to operators, or marine life.
E. A visual feedback system that indicates the current state of the system, Estop, Manual, Autonomous.
F. The vehicle must be positively buoyant and float to the surface when power is removed from the propulsion system.

2) Autonomy demonstration strategy: Team Minion's autonomy demonstration strategy was developed to satisfy the challenge requirements through a straightforward and achievable approach while minimizing the development time required to meet the submission deadline. This section outlines the intended demonstration procedure and identifies the capabilities necessary for its completion. The autonomy strategy is also shown in Fig. 3.

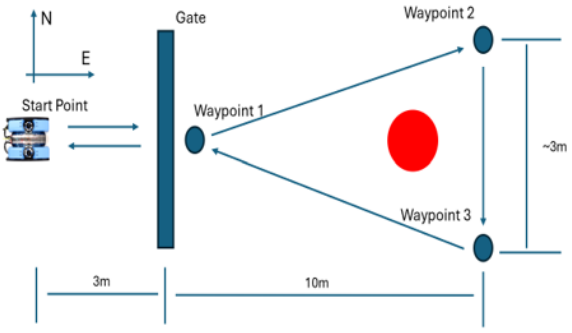


Fig. 3: Waypoint structure of autonomy strategy.

The plan is to form a predefined list of 5 waypoints consisting of the start location, the gate forward location (Waypoint 1), and two waypoints to navigate around the buoy (Waypoints 2 and 3). First the vehicle will be placed at the start location. Second the vehicle will dive to the depth of the gate and will navigate forward to waypoint 1. Next the vehicle will travel to Waypoint 2 positioned counter-clockwise away from the marker to avoid a collision. Next the vehicle will navigate to waypoint 3 on the opposite side of the marker, then back to Waypoint 1 and lastly, return to the start point, the 5th and final waypoint. The UUV is a holonomic vehicle so the straight line paths can be achieved by simple waypoint following. The guided mode of the controller at distances less than $5\,\mathrm{m}$ will slew heading and distance error meaning in some motions the vehicle will strafe towards the waypoint rather than executing a turn and drive maneuver. For this implementation waypoints are two dimensional, x and y positions. For later competition development ArduPilot will need to be reconfigured to enable more rigorous heading control.

To achieve this the vehicle will need to be able to perform a few core capabilities. First the vehicle needs to be watertight at pressures down to $5\,\mathrm{m}$ since the autonomy demonstration takes place in a pool no more than $5\,\mathrm{m}$ deep, which is an apparent pressure of 1.5 atmospheres. Second the vehicle needs to be capable of safely powering all of its components without external power. Third the vehicle needs to communicate with a ground station to accept mission start and end commands. Next the vehicle needs to accurately localize its position over a period of less than $5\,\mathrm{min}$. Finally the vehicle needs to be capable of reaching its intended waypoints.

3) The platform: The team chose to purchase a pre-built platform to speed up development of the system, given the short 6-month development timeline. Previous teams have utilized pre-built platforms for RobotX primarily to gain initial experience with subsurface operation of autonomous vehicles. The team's selection of ROV Maker components was further supported by their successful use by other competition teams, providing confidence in their suitability for the RobotX operating environment [11]. In the challenging environment that the RobotX competition environment poses, a prebuilt and verified platform provided the team with a confident starting point with which to begin development.

The BlueROV2 Heavy platform automatically addresses safety requirements D and F. The Heavy comes with non-compressible floats made from R-3318 closed cell foam. These will maintain their shape, and buoyancy at depth providing reliable additional buoyancy to conform to weight changes made during development to ensure the vehicle is positively buoyant. Fig. 4 shows the weight budget drawn up for the vehicle revealing that there is 13.95 lb of margin in buoyancy.

The platform also ships with eight T200 motors, powerful marine electric motors suitable for the size of the vehicle. Four of the motors point downwards providing Z axis control. The T200 motors can produce 3.5 kgf of thrust each. A total of 30.8 lbf of thrust is suitable to submerge the platform in a configuration with the floats attached. An additional feature of the T200 motors is the built-in shrouding. The protective cowling around the motors services requirement D that the propulsion system is safe for operators and marine life.

The Blue Robotics BlueROV2 Heavy is designed for underwater applications such as monitoring industrial equipment, environmental monitoring or marine research. The vehicle is built to operate as a piloted craft with video and telemetry

Weight Budget			
Weight		Buoyancy	
Component	Weight (lbs)	Component	Displacement (lbs)
BlueROV2 Heavy	26	Floats	8
Tow Points	1.86	Battery Enclosure	4.77
Faceplate Assembly	1.7	Electronics Enclosure	14.85
Battery	2.6	Frame	26.79
Periscope	2	Periscope	1.3
DVL + Ping 360	2		
Electronics Enclosure	5.6		
Total (lbs):	41.76	Total (lbs):	55.71
Net Buoyancy		Total (lbs):	13.95

Fig. 4: Weight budget of Jit.



Fig. 5: T200 motor with shrouding [12].

sent back to a ground station via a tether for recording and observation by a pilot. The sensor suite, provided on the Navigator board of the system, is sufficient for piloted operation. The Navigator board is capable of reporting yaw, pitch, and roll based on the magnetometer and constant gravity vector, enough to create an accurate to 1° to 2° navball and heads up display for pilot orientation. The camera feed is streamed back to a ground station at 1080p and 30 frames per second. These sensors are not capable of providing a stable horizontal position estimate to support the autonomy goals, which necessitated the physical redesign of the platform. A main goal for our autonomy scheme relies on effective localization of the vehicle in its local frame. To achieve this while submerged more reliable position estimation was needed than can be provided by the inertial sensors on the Navigator board. The Water Linked DVL is officially supported by ArduSub and provides a more reliable linear error source for horizontal localization. For these reasons the A50 DVL was chosen. The team sourced an additional high-end sensor for use on the vehicle, a Blue Robotics Ping 360 scanning sonar for situational awareness in murky waters. These sensors, the Ping 360 and DVL have seen broad use by other RoboSub and RobotX teams. To accommodate the increased computational power required of an autonomous platform an additional Raspberry Pi 4 was added to the electronics enclosure. The provided Raspberry Pi runs BlueOS, Blue Robotics' custom ROV operating system. That computer was nearing its limits of capabilities while managing the provided sensors, camera, and DVL. Adding additional compute requirements to the provided Pi such as processing sonar inputs, communications, and autonomy functions was deemed unreliable from the team's initial testing of the computer as buffering and stuttering of inputs was observed with just the sonar connected. Additionally, the Pi as delivered did not easily support ROS 2, the team's preferred software framework for autonomy. To spread the computational requirements and facilitate easier development the team decided that an additional Raspberry Pi, known as the companion computer, was required.

D. Modifications

1) Mechanical redesign: The stock BlueROV2 Heavy includes a four-inch-diameter, 12-inch-long acrylic tube for housing the electronics. But this electronics enclosure did not have room for expansion, which is needed for adding connections and power distribution to the new sensors, and the computing hardware to process their data. To accommodate an additional Raspberry Pi, two sensors and communication hardware, a new enclosure was needed. A five-inch diameter 16-inch-long acrylic tube from ROV Maker was purchased, and the chassis was redesigned to accommodate the larger tube. Later, to accommodate battery safety systems, the original electronics enclosure was repurposed to serve as the battery enclosure.



Fig. 6: Redesign of chassis and new orientation.

The larger tube was originally intended to be mounted to the underside of the chassis, but initial flotation testing revealed that the UUV would be unstable. The system was then reconfigured to operate in an inverted configuration. The dive motors were inverted, and the autopilot was configured to operate upside down. This had the additional benefit of lowering the resting location of the dive motors resulting in more initial vertical control due to reduced cavitation.

The larger tube from ROV Maker is like the Blue Robotics enclosure but lacks a locking endcap. The Blue Robotics enclosure includes a plastic tube which feeds into a slot in the

aluminum end cap and acrylic tube. This lock ring serves to prevent the end cap assembly from being removed by force. Unfortunately, Blue Robotics does not offer a large enough acrylic tube with a lock ring, so the ROV Maker tube was selected. During testing the end cap of the larger tube was inadvertently pulled off resulting in the electronics enclosure flooding. To prevent this from occurring a new faceplate was designed. The faceplate in Fig. 7 is manufactured out of 316 stainless steel and is 3/16 in thick, which closely matches the $4\,\mathrm{mm}$ aluminum cap purchased from ROV Maker. The threaded rods joining the two faceplates will effectively clamp the end caps in place with lock nuts preventing unintentional removal.



Fig. 7: Modified faceplate assembly.

To satisfy requirement B the team designed tow points for moving and transporting the vehicle by external power. The tow points needed to be strong enough to withstand the loads applied through the tow lines, including the worst case in which the motors unintentionally fire while the tow lines are attached. The four lateral motors can produce a maximum thrust of 9.9 kgf in line with the tow point. The tow points are made from the same 316 stainless steel plate used for the modified faceplate, which has a yield strength of $290\,\mathrm{MPa}$. The maximum stress experienced by a single tow point will be $683\,\mathrm{kPa}$ at the weakest cross section. In simple tension the factor of safety is 424.47 for one tow point in the worst case scenario.

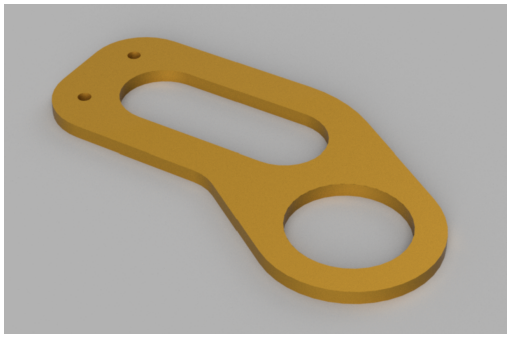


Fig. 8: Tow point.

2) Electrical: A battery was needed to provide sufficient current and endurance to the UUV. To find this battery, the team began by determining the system power requirements during the RobotX competition. The below operational analysis aimed to quantify the average power draw of the vehicle over the course of one competition run of approximately $30\,\mathrm{min}$. The values for time in each state are meant to reflect anticipated time in each operating mode. The values for wattage are sourced from Blue Robotics' own resources for the T200 motor [12].

Operational Analysis Total Time 30 Mins					
Movement Types	# of Thrusters	Time Mins	Percent	Wattage @ 14V	Total Wattage
Idile	0	10	33.3%	10.7	0.0
Surface Hold	4	5	16.7%	5.3	21.3
Surface Drive	4	5	16.7%	5.3	21.3
Submerge Hold	8	2	6.7%	2.1	17.1
Submerge Drive	8	8	26.7%	8.5	68.3
				Total W:	128

Fig. 9: Operational analysis of Jit during competition.

The team selected the Blue Robotics Li-4S-18A R1 battery for the vehicle due to its price point, size, and compatibility with the repurposed enclosure [13]. This battery under the anticipated load will provide over two hours of run time. Additionally, a load analysis of the other sensors and systems was conducted and found to be insignificant to the needed runtime requirements.

BATTERY					
Pack	Qty	V	Cap (Ah)	E (Wh)	C Rate
Blue Robotics Li-4S-18A	1.0	14.8	18.0	266.4	2.1
				EST. RUNTIME (Min)	124.9

Fig. 10: Load analysis of selected battery.

To satisfy requirement A for the Estop system the team developed a simple system that has two independent methods of removing motor power: the physical switch and the remotely activated switch. To do so, the internal wiring of the electronics enclosure is divided into two main battery power buses with independent lines running from the battery enclosure to the electronics enclosure. A single-pole, single-throw nominally open relay is placed in line with the high side of the motor power bus. The relay coil is powered by battery voltage connected to a single-pole locking switch. As per the requirements, a red $3\,\mathrm{cm}$ cap is attached to the purchased marine grade switch. The switch is placed on the faceplate of the battery enclosure. In series with the physical Estop switch is a nominally open signal driven relay. Fig. 11 shows a simplified diagram of the working system. On start up the motors do not receive power. The companion computer waits to receive a signal from the RC remote. When switched to active mode the Pi will pull pin 2 of the remote relay high which is attached to the signal line of the remote relay closing the circuit. The coil line has a $3.3\,\mathrm{V}$ LDO tap used as a feedback line to the companion computer to control the indicator lights. This LDO feedback is needed to update the external indicator of state, per requirement E.

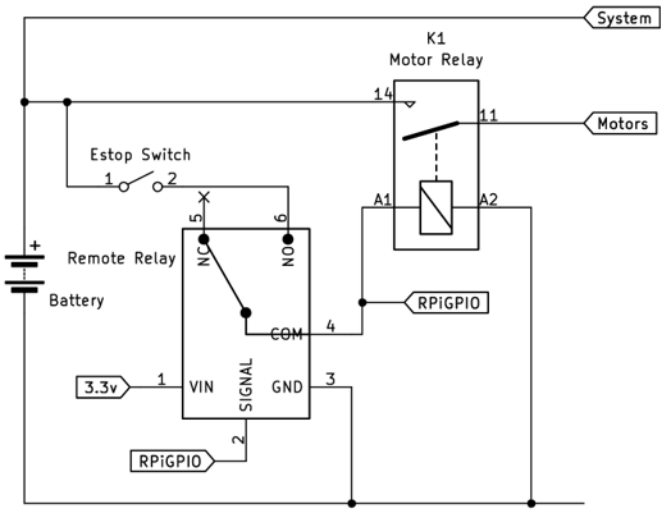


Fig. 11: Estop circuit diagram.

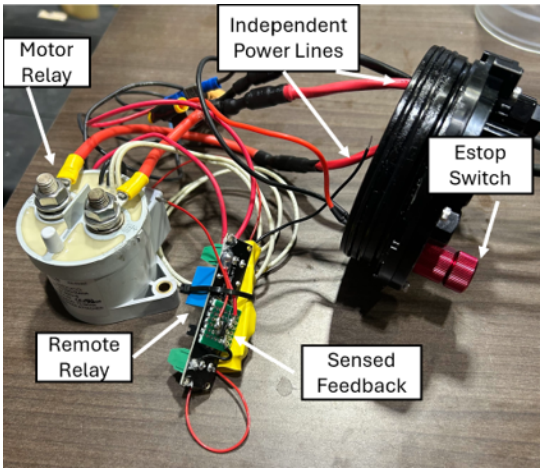


Fig. 12: Estop hardware.

The remote Estop functionality was validated by bench testing the system. This started with the remote relay and MicroRx receiver connected to the companion computer. When the Estop channel is activated the remote relay responds and opens the circuit and no noticeable delay between input and actuation was observed, even under load. The light panel logic is largely driven by the system monitor's state, however if the LDO line ever goes low the logic will turn the LEDs red regardless of activated control state. The input pins of the RPi are configured with input resistors, but as a precaution an additional current limiting resistor is placed on the feedback line.

Fig. 13 shows the maximum-load analysis of the vehicle's motor system. The maximum anticipated current of the motors is 168 A. The kill switch relay, the EV200HAANA, is rated for switching up to 250 A. The ERAU RoboSub team also uses 8 T200 motors on their custom UUV HammerHead and sized their Estop relay at 250 A [14]. During preliminary testing the vehicle experienced a runaway failure where the Estop was triggered and performed as expected. The components likely to be harmed by flyback current, the ESCs, were each tested after the event and showed no signs of damage.

MAXIMUM LOAD						
Component	Qty	Duty	V	I (A)	I Total (A)	P (W)
Motors	8	100%	14.8	21	168	2486.4

Fig. 13: Load analysis of motor system at max.

3) Thermal management: The BlueROV2 Heavy does not include an active thermal-management system in its standard configuration. During testing, several onboard processes exhibited reduced performance as a result of CPU thermal throttling. To address this issue, three cooling fans were added to the electronics enclosure. One fan is aligned with the heatsink on each Raspberry Pi, while the third promotes general airflow throughout the enclosure. Although the outdoor temperatures encountered during testing in Florida are expected to be slightly higher than those anticipated in Singapore during the competition, these additions are intended to improve overall system reliability and reduce the risk of heat-related performance degradation. The thermal management solution was bench tested with the companion computer and BlueOS computer powered on and fans placed in line with the heatsinks. The core temperature on both systems remained stable and well below their operating maximum. The thermal-management system will be evaluated during further testing while local environmental conditions remain representative of those expected in Singapore in November.

4) Software: The primary software objective was to extend the existing BlueROV2 control architecture with ROS 2 while retaining ArduSub for low-level vehicle control and state estimation. In the original configuration, the Navigator autopilot communicates with the provided Raspberry Pi 4B running Blue Robotics' BlueOS. BlueOS manages communication between the autopilot, DVL, and external systems while providing interfaces for autopilot configuration, sensor calibration, controller parameters, software packages, communication endpoints, and video streams. Initial bench testing also indicated that the Raspberry Pi running BlueOS was approaching its available computational capacity.

To provide additional processing resources and reduce the load placed on the BlueOS computer, the team integrated a second Raspberry Pi 4B running Ubuntu 22.04 and ROS 2 Humble. A Raspberry Pi 5 was initially considered for its increased performance, but the Raspberry Pi 4B was selected to maintain compatibility with the team's existing messages on ROS 2 Humble and reduce the additional development required for integration.

Communication between BlueOS and the ROS 2 companion computer was established through a MAVLink endpoint configured using the BlueOS endpoint manager. MAVROS was then used to receive ArduSub data and expose the available telemetry, state estimates, and services as ROS 2 topics and services. This architecture preserved the existing BlueOS and ArduSub functionality while allowing higher-level autonomy and sensor-processing tasks to be performed on the companion computer. A Blue Robotics Ping 360 scanning sonar was also integrated into the system to support future underwater

mapping processes for the competition task. This is however out of the scope of the proof of readiness task.

Reliable local position estimation was required to support waypoint navigation during the autonomy demonstration. To meet this objective, the team configured ArduSub's EKF3 estimator to combine measurements from the onboard inertial sensors, depth sensor, magnetometer, and Water Linked A50 DVL. After proper calibration, static localization performance was evaluated. The vehicle exhibited approximately $10\,\mathrm{cm}$ of horizontal drift over five minutes, heading oscillations of approximately 1° to 2°, and stable depth estimates. The addition of DVL velocity measurements qualitatively improved the stability of the horizontal position estimate. The DVL produces vehicle velocity estimates which the Navigator integrates for position. A constant velocity bias produces position error that grows approximately linearly with time, whereas a constant acceleration bias can produce position error that grows quadratically with time. Dynamic localization performance has not yet been characterized and is expected to be affected by vehicle motion, motor-induced magnetic interference, and increased inertial-sensor noise. This will however be sufficient over short periods as seen by other RoboSub teams.

Sensor calibration was also found to be strongly influenced by the surrounding environment. Early magnetometer calibrations were performed near a metal shelter and table, where magnetic interference caused inconsistent north references and persistent heading drift when the vehicle was moved to the pool. This issue was resolved by conducting calibration away from large metallic structures, reducing the effects of magnetic offsets and producing more consistent heading estimates.

5) Communication: The UUV will communicate with external systems through a Ubiquiti bullet Wi-Fi antenna, and a betaFPV micro ELRS receiver. These components along with a Ublox GNSS module were placed in a dedicated enclosure known as the *periscope*. The periscope is a two-inch diameter acrylic enclosure purchased from Blue Robotics. The Ublox GNSS module will provide the vehicle with accurate localization while on the surface and with a clear view to the sky. The module has a reported 50% circular error probable (CEP) of $2.5\,\mathrm{m}$ on the GPS constellation [15]. The MicroRx receiver enables manual control of the vehicle and remote Estop capability separate from a ground station computer as per requirement C. The bullet antenna enables wireless operation of autonomy functions through a ground station computer for testing and logging. The antenna additionally enables communication with Team Minion's USV. This capability allows the USV to transmit obstacle information and path planning waypoints to guide Jit to the task location during competition.

6) LED indicator lights & RC control: To satisfy requirement C the team has built an RC control system to manually pilot the vehicle, remotely activate the Estop, and update the indicator lights. The current hardware supports sensed feedback of the Estop line seen in Figs. 11 and 12, and an internal status monitor node will keep track and update the light panel on the vehicle's control state. Additionally, hardware and software to support transmitting RC controls to ROS topics have already been created. The Rx interpreter node recasts the serial channel values from the Micro Rx to individual topics that can be sent to the BlueOS computer with MAVROS. Fig. 15 is a simplified functional diagram of the RC and indicator light system.



Fig. 14: Periscope communication hardware.

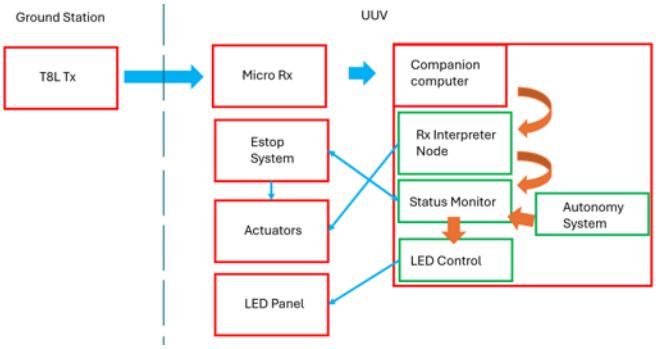


Fig. 15: Functional block diagram of RC & indicator light system.

A multi-LED RGB panel is fitted to the threaded rods of the faceplate modification. Fig. 16 shows the light panel used on Jit, which consists of a rigid back plate supporting the LED panel and an acrylic cover bolted to the face. The panel is potted in epoxy for sealing.



Fig. 16: JIT light panel.

E. Competition Autonomy Plan

To achieve the minimum viable functionality required for the competition, Jit must be capable of navigating to the underwater task location, communicating with the USV, and completing a basic inspection pass. The proposed operational sequence is shown in Algorithm 1. The USV is responsible for identifying the task location and generating a safe surface path, while the UUV is responsible for following the transmitted path, diving at the task location, and recording sonar data.

Algorithm 1 Minimum Viable UUV Task Execution

Inputs: USV course map, detected buoy locations and colors, surfaced UUV position.
Output: UUV navigation path and recorded sonar data

1: **Map the course.** While the USV completes tasks the USV creates a map of the competition area classifying objects.
2: **Identify the target buoys.** From the mapped buoy detections, select the red and green buoys that display a constant, non-flashing color.
3: **Generate a path.** USV path planner generates an obstacle free path using the surfaced UUV's start position as the start and the selected green buoy as the goal.
4: **Transmit the path to Jit.** The generated waypoints are sent to Jit through wireless communication network.
5: **Navigate to the path.** Jit follows the transmitted path on the surface using GNSS-based localization.
6: **Perform submerged pass.** At the task location, Jit dives to a preset depth and traverses along the pipeline, from the green buoy to the red buoy in a straight line, while recording data from the Ping 360 sonar. After a set distance the vehicle surfaces.

Target identification relies on the infrastructure-inspection buoys displaying a constant color rather than a flashing one. From the buoy detections in its course map, the USV selects the red and green buoys with a steady color as the inspection pair. The green buoy then serves as the goal for path planning, and Jit performs its submerged pass from the green buoy to the red buoy. The exact implementation of this process will depend on the buoy detection and mapping information available from the USV.

F. Conclusion

Jit represents Team Minion's return to underwater vehicle development for the 2026 RobotX Maritime Challenge. By modifying a Blue Robotics BlueROV2 Heavy, the team established a hardware and software platform intended to support autonomous navigation, wireless communication, localization, and competition-required safety functions. The redesigned vehicle includes an expanded electronics enclosure, ROS 2 companion computer, additional navigation sensors, and physical and wireless Estop capabilities. Initial testing identified several challenges, including localization drift, thermal management, sensor calibration, enclosure sealing, and command reliability.

REFERENCES

[1] Team Minion, "Design of the Minion research platform for the 2018 Maritime RobotX Challenge," Embry-Riddle Aeronautical University, Daytona Beach, FL, USA, Tech. Rep., 2018. [Online]. Available: https://robonation.org/app/uploads/sites/2/2019/09/ERAU_RX18_Paper.pdf. Accessed: Jul. 10, 2026.

[2] RSS, "RobotX Team Handbook." [Online]. Available: https://robonation.gitbook.io/robotx-2026-team-handbook. Accessed: Aug. 1, 2026.

[3] Team QUT, "Bruce: A system-of-systems solution to the 2018 Maritime RobotX Challenge," Queensland University of Technology, Brisbane, Australia, Tech. Rep., 2018. [Online]. Available: https://robonation.org/app/uploads/sites/2/2019/09/QUT_RX18_Paper.pdf. Accessed: Jul. 11, 2026.

[4] Team Owltonomous, "Team Owltonomous RobotX journal paper 2018," Florida Atlantic University, Boca Raton, FL, USA, Tech. Rep., 2018. [Online]. Available: https://robonation.org/app/uploads/sites/2/2019/09/FAU_RX18_Paper.pdf. Accessed: Jul. 11, 2026.

[5] Team Bumblebee, "Bumblebee Autonomous Surface Vessel 2.0 Technical Design Paper 2018 RobotX Competition," National University of Singapore, Tech. Rep., 2018. Accessed: Aug. 04, 2026. [Online]. Available: https://bumblebee.sg/pdf/NUS-Team-Bumblebee-RobotX-2018-Technical-Paper.pdf

[6] Blue Robotics, "BlueROV2 assembly and build instructions." [Online]. Available: https://bluerobotics.com/learn/bluerov2-assembly/. Accessed: Jul. 31, 2026.

[7] RSS, "RoboSub Team Handbook." [Online]. Available: https://robonation.gitbook.io/robosub-resources. Accessed: Jul. 31, 2026.

[8] BRACU Duburi, "BRACU Duburi AUV technical design report," BRAC University, Bangladesh, Tech. Rep., 2025. [Online]. Available: https://robonation.org/app/uploads/sites/4/2025/07/RS25_TDR_BRAC-University-Duburi_compressed.pdf Accessed: Jul. 27, 2026.

[9] Team DAVE, "Desert WAVE: Women in Autonomous Vehicle Engineering," Arizona State University, AZ, USA, Tech. Rep., 2025. [Online]. Available: https://robonation.org/app/uploads/sites/4/2025/07/RS25_TDR_Arizona-State-Si-Se-Puede-Desert-WAVE.pdf. Accessed: Jul. 24, 2026.

[10] Team All Blue, "RoboSub 2025 technical design report," Universidade de Brasília, Brasília, Brazil, Tech. Rep., 2025. [Online]. Available: https://robonation.org/app/uploads/sites/4/2025/07/RS25_TDR_Universidade-de-Brasilia-AllBlue.pdf. Accessed: Jul. 28, 2026.

[11] Team DOB HydroJan, "HydroJan 1.0—Technical design report, Dreams of Bangladesh—RoboSub 2025," Dreams of Bangladesh, Tech. Rep., 2025. [Online]. Available: https://robonation.org/app/uploads/sites/4/2025/07/RS25_TDR_Dreams-of-Bangladesh-HydroJan.pdf. Accessed: Jul. 28, 2026.

[12] Blue Robotics, "T200 thruster." [Online]. Available: https://bluerobotics.com/store/thrusters/t100-t200-thrusters/t200-thruster-r2-rp/. Accessed: Aug. 4, 2026.

[13] Blue Robotics, "Lithium-ion battery (14.8 V, 18 Ah)." [Online]. Available: https://bluerobotics.com/store/comm-control-power/powersupplies-batteries/battery-li-4s-18ah-r3/. Accessed: Aug. 1, 2026.

[14] Team Unsinkable, "HammerHead AUV technical design report," Embry-Riddle Aeronautical University, Daytona Beach, FL, USA, Tech. Rep., 2025. [Online]. Available: https://robonation.org/app/uploads/sites/4/2025/07/RS25_TDR_Embry-Riddle-AMRA-Team-Unsinkable.pdf. Accessed: Jul. 17, 2026.

[15] SparkFun Electronics, "SparkFun GNSS receiver—SAM-M8Q (Qwiic)." [Online]. Available: https://www.sparkfun.com/sparkfun-gnss-receiver-sam-m8q-qwiic.html. Accessed: Aug. 4, 2026.

Appendix D: Systems Engineering Approach for E-Stop System Design for Uncrewed Surface Vessels

Sarthak Aggarwal

I. Purpose and Context

Emergency-stop (E-Stop) systems are a non-negotiable safety requirement for Uncrewed Surface Vessels (USVs), yet existing commercial and consumer solutions are poorly suited for educational and research platforms. This appendix documents the systems engineering process behind a dedicated E-Stop printed-circuit board developed for *EasyUSV*, an educational kit that lets high-school and college students build USVs meeting the safety requirements of student competitions such as RoboBoat and the Maritime RobotX Challenge. The design is governed by ISO 13850 [1] and implements *Category 0* (immediate, hardwired cutoff) and *Category 1* (controlled stop) response modes. A Failure Modes and Effects Analysis (FMEA) was conducted across ten fault categories and 73 fault modes, with each scored using a Risk Priority Number $\mathrm{RPN} = L \times S$ and every mitigation classified as hardware (**H**), firmware (**F**), or documentation (**D**).

A. Motivation for a dedicated E-Stop

Delegating the E-Stop function to existing vessel subsystems – the autopilot's arming logic or the ESC's signal-loss behavior – fails on three counts. First, any cutoff sharing a fault domain with the system it protects is vulnerable to the same failures (a firmware crash, a corrupted mission state, an unresponsive autopilot cannot reliably command its own shutdown). Second, marine propulsion on a USV of this class operates at 12–30 V and draws tens of amperes under load, a power domain logic-level GPIO and consumer-grade ESC inputs are not designed to interrupt deterministically. Third, a safety-critical system must be *fail-safe by construction*: the default state under loss of power, loss of comms, or undefined firmware behavior must be propulsion-disabled, regardless of what the mission software believes. A dedicated E-Stop PCB, electrically and logically independent from the autopilot stack, satisfies all three requirements directly.

B. Requirements

RoboBoat [2] and RobotX [3] both mandate an operator-accessible remote emergency-stop with demonstrable fail-safe behavior under loss of comms or operator control. ISO 13850 [1] further requires that recovery demand a deliberate manual reset and that the stop function not substitute for other safeguards. Combined with the educational-kit context:

- **R1 – Remote activation:** triggerable by a field operator without physical contact with the vessel.
- **R2 – Local activation:** also triggerable by a physical button on the vessel.
- **R3 – Actuator cutoff:** activation removes power from all actuators, including propulsion, independent of autopilot or mission software.
- **R4 – Fail-safe default:** loss of power, loss of comms, or undefined firmware behavior defaults to propulsion-disabled.
- **R5 – Manual reset:** recovery requires deliberate operator action; the system does not self-restore.
- **R6 – Ease of integration:** keyed connectors, documented pinouts, standard tooling, minimizing wiring errors by builders without marine-electronics experience.
- **R7 – Diagnostic visibility:** unambiguous indication of armed, triggered, and fault states to both builder and operator.

R1–R5 derive from competition rules; R6–R7 are specific to the educational context. These requirements anchor the FMEA mitigations (§III) and the validation plan (§IV).

C. E-Stop categories per ISO 13850

Category 0 is an immediate, hardwired removal of power – no software in the loop, motion ceases uncontrolled. This is the default safe state, invoked under loss of comms, loss of MCU heartbeat, or brownout of the board's own supply. **Category 1** is a controlled stop: power is maintained only long enough for firmware to bring the vessel to a halt, then removed, invoked during nominal operator-initiated stops to reduce mechanical stress and avoid wake-induced motion. **Category 2** (controlled stop with power maintained, per IEC 60204-1 [4]) is not a valid emergency-stop response, since it leaves hazardous energy available on the actuators. The current design implements Category 0 only – the low-inertia propulsion of student-scale USVs does not carry enough kinetic energy during nominal operation to justify the added complexity of a controlled ramp-down.

II. Literature Review

A. ISO 13850 overview

Beyond the category taxonomy above, ISO 13850 specifies: the stop device shall be a palm- or mushroom-type actuator, red on yellow, with direct-opening action; the actuator shall latch on activation; recovery shall require a deliberate, separate reset action; and the E-Stop is a complementary protective measure, not a substitute for other safeguards. The standard excludes the stopping *method* (reversal, emission deflection, braking) from its scope, leaving that to complementary standards such as IEC 60204-1 [4].

B. Precedents

Industrial safety relays (Pilz PNOZsigma/PNOZ X, certified to IEC 62061 and ISO 13849-1 up to PL e [5]) are a poor match for this application: designed for fixed-installation, mains-voltage machinery, not weather-sealed, and at $200–$600 per relay [5] approach or exceed the entire target BOM cost. Consumer RF kill switches address cost and voltage but lack documentation and ISO 13850's latching/reset requirements. Prior academic work on wireless E-Stop for mobile robots [6] is architecturally similar but not marine-specific and publishes no reproducible reference design. RoboBoat/RobotX team Technical Design Reports [7], [8], [9] consistently treat E-Stop as mandatory, but each team builds a bespoke design with no shared reference architecture or BOM – the specific gap this work addresses.

C. Technical foundations

The FMEA methodology (§III) follows IEC 60812 [10]. Firmware practices – watchdog timers, fail-safe default outputs, ISR atomicity – are grounded in IEC 61508 [11] and standard embedded-systems literature [12]. USV-specific safety literature operates mostly at the mission/formation level (e.g. Wang *et al.*'s SysML/STPA hazard analysis for USV formations [14]); subsystem-level safety-function design for small USVs, including actuator cutoff architectures for student and research platforms, remains comparatively unaddressed – the narrower domain this work contributes to.

III. FMEA Methodology

Failure modes were enumerated across ten functional categories (Table I) and rated by a panel of three subject-matter experts spanning marine hardware, autonomous-vehicle safety, and competition USV development. Each expert independently assigned Likelihood (L) and Severity (S) on a 1–5 ordinal scale (Table II); where ratings diverged, the value from the most experienced respondent was adopted.

$$\mathrm{RPN} = L \times S, \quad L, S \in \{1, 2, 3, 4, 5\}, \tag{1}$$

giving integer RPN on $[1, 25]$, banded into four risk levels with a recommended action per band (Table III). Only faults with $\mathrm{RPN} \geq 10$ are discussed individually below; lower-band faults are handled by standard engineering practice. Each fault is paired with mitigations tiered as **(H)** hardware (schematic, layout, component, enclosure), **(F)** firmware (ESP32-S3 logic), or **(D)** documentation (assembly guide, checklist) – supporting traceability from fault to deliverable and, in §IV, to an acceptance test. Any fault with $S = 5$ (catastrophic) is flagged for explicit treatment regardless of likelihood.

A. Power supply faults (PWR)

Nine PWR faults were identified covering input conditioning, regulation, and protection (Table IV).

The dominant high-band fault is **PWR-02**: a sustained input sag below the MCU's operating threshold that fails to trigger a clean reset, leaving GPIO outputs in an indeterminate state and directly violating R4 – common on battery-powered platforms,

TABLE I: FMEA fault categories, one per subsection below.

ID	Category	§
PWR	Power supply	A
BTN	E-Stop button / loop integrity	B
OUT	Output driver / contactor	C
MCU	Microcontroller and firmware	D
COM	Communications	E
HMI	Human-machine interface	F
CON	Connectors and wiring	G
ENVR	Environmental	H
SYS	System-level	I
HUMN	Human factors	J

TABLE II: Likelihood (L) and Severity (S) rating rubrics, 1–5 ordinal scale.

Likelihood of Occurrence (L)		
1	Very Unlikely	No known precedent; requires multiple independent failures.
2	Unlikely	Theoretically possible, rare with proper design practice.
3	Occasional	Observed in comparable systems; a few times over vessel lifetime.
4	Likely	Common failure mode without specific countermeasures.
5	Frequent	Almost certain during typical use.
Severity of Outcome (S)		
1	Negligible	No safety implication, no loss of vehicle control.
2	Minor Mission Impact	Non-critical capability lost; vehicle stays safe/controllable.
3	Mission Loss	Vehicle can still reach a safe state (e.g. controlled shutdown).
4	Hazardous Operation	Vehicle may operate unsafely; risk of damage or injury.
5	Catastrophic	Loss of control, high likelihood of serious injury/damage.

TABLE III: Risk Priority Number bands and recommended actions. Color coding applied consistently across all FMEA tables below.

RPN	Level	Recommended Action
1–4	Low	Accept without additional mitigation.
5–9	Medium	Mitigate if low-cost, else monitor during testing; escalate to High if repeated.
10–16	High	Specific design change, safeguard, or documented control required before deployment.
17–25	Critical	Unacceptable residual risk; board shall not ship unmitigated.

TABLE IV: Power Supply (PWR) faults. Color coding follows Table III.

ID	Fault	L	S	RPN	Mit.
PWR-01	Complete loss of input power	2	3	6	H
PWR-02	Brownout, no proper reset	4	4	16	H, F
PWR-03	Overvoltage at input	2	4	8	H
PWR-04	Reverse polarity, protection fails	2	3	6	H
PWR-05	Transient-induced MCU latchup/reset	3	3	9	H
PWR-06	Regulator fails with high output	1	4	4	H
PWR-07	Regulator fails low, partial power	3	3	9	H, F
PWR-08	EMI coupling to logic rails	3	3	9	H
PWR-09	Bulk capacitor degradation	2	3	6	H

where discharge sag can fall between the battery's undervoltage cutoff and the MCU's brownout-detect threshold. The mitigation is a two-stage voltage-sense scheme. **(H)** A resistor divider on V_{IN} feeds an ADC input, with cutoff threshold

$$V_{\mathrm{th}} = V_{\mathrm{min}} \cdot \frac{R_1 + R_2}{R_2}, \tag{2}$$

where V_{min} is the minimum acceptable rail voltage at the MCU; an ideal-diode controller at the input provides reverse-polarity protection (also mitigating PWR-04). **(F)** The sensed voltage is reported to the main computer for early operator recovery, and when V_{IN} crosses V_{th} the firmware asserts a Category 0 cutoff before the MCU loses the ability to command its own shutdown.

B. E-Stop button / loop faults (BTN)

Eight BTN faults cover the physical actuator, sensing loop, and board-side input conditioning (Table V).

TABLE V: E-Stop Button and Loop (BTN) faults. Color coding follows Table III.

ID	Fault	L	S	RPN	Mit.
BTN-01	Open loop not detected, reports OK	3	4	12	H
BTN-02	Loop accidentally shorted closed	2	3	6	H
BTN-03	Button sense pin stuck high/low	2	4	8	H
BTN-04	Wrong pull-up/pull-down value	1	4	4	H
BTN-05	Contact bounce confuses firmware	2	3	6	H, F
BTN-06	Long-cable ground-potential shift	2	3	6	H
BTN-07	Salt-water leakage path on sense	1	3	3	H, D
BTN-08	Latch wear, spontaneous release	3	4	12	H, D

Both high-band faults are addressed by topology/component selection rather than firmware. **BTN-01** (undetected open loop) is mitigated by wiring the button as a *normally-closed* current loop: a broken wire, unseated connector, or corroded contact breaks the loop, which the board reads as a pressed E-Stop – inverting the default failure mode from "fail-silent" to "fail-safe" and satisfying R4 without firmware needing to distinguish a press from a broken connection. **(H)** Hardware debounce (RC network plus Schmitt-trigger buffer) suppresses mechanical bounce (BTN-05) before the MCU sees it. **BTN-08** (latch wear) is mitigated by **(H)** an IP65-rated stainless-steel mushroom-head actuator rated for 10^5 cycles, and **(D)** an annual inspection interval plus a pre-launch latch-engagement check.

C. Output driver / contactor faults (OUT)

Ten OUT faults cover the path from MCU control signal to the propulsion power contactor: the low-side MOSFET driver, the flyback path, and the contactor itself (Table VI).

The three high-band faults share an outcome – cutoff fails closed, propulsion stays energized – but split into two

TABLE VI: Output Driver and Contactor (OUT) faults. Color coding follows Table III.

ID	Fault	L	S	RPN	Mit.
OUT-01	Driver fails OFF, no actuation	3	2	6	H
OUT-02	Driver fails ON, cannot de-energize	2	5	10	H, F
OUT-03	MOSFET drain-source short	2	5	10	H, F
OUT-04	Open driver circuit, cracked trace	1	1	1	H
OUT-05	Flyback diode open, inductive kick	2	3	6	H
OUT-06	Flyback diode shorted	2	3	6	H
OUT-07	Contactor contacts welded shut	2	5	10	D
OUT-08	Contactor mechanically jammed	2	4	8	D
OUT-09	Feedback signal missing/broken	3	3	9	H, F
OUT-10	Coil thermally degraded	1	3	3	D

mechanisms. **OUT-02/OUT-03** (stuck-on MOSFET) are mitigated by **(H)** a low-side switch topology with a gate pull-down sized to dominate GPIO leakage current (default OFF), plus a Schottky flyback diode clamping the turn-off transient $V_{\mathrm{spike}} = L_{\mathrm{coil}}(dI/dt)$ (also addressing OUT-05); **(F)** a power-on self-test verifies expected coil-current draw before reporting armed, with missing/inconsistent feedback (OUT-09) itself blocking arming. **OUT-07** (welded contacts) is a mechanical reliability failure independent of the driver, mitigated by **(D)** a documented contactor selection rule: rated continuous and inrush current shall meet a **1.5× safety margin** over maximum expected draw, extended to OUT-08 and OUT-10.

D. Microcontroller / firmware faults (MCU)

Nine MCU faults cover firmware logic and the firmware/hardware boundary: watchdog behavior, boot-time defaults, interrupt handling, runtime state integrity (Table VII).

TABLE VII: Microcontroller and Firmware (MCU) faults. Color coding follows Table III.

ID	Fault	L	S	RPN	Mit.
MCU-01	MCU crash or infinite loop	2	4	8	F
MCU-02	Watchdog not enabled	1	3	3	F
MCU-03	Watchdog timeout too long	3	4	12	F
MCU-04	Logic bug, missed E-Stop condition	2	3	6	F
MCU-05	Boot defaults energize contactor	4	3	12	H, F
MCU-06	Flash corruption, bad firmware	2	2	4	F, D
MCU-07	Clock or oscillator drift	3	1	3	F
MCU-08	ISR race overwrites E-Stop state	2	5	10	F
MCU-09	Stack or heap overflow	1	3	3	F

The three high-band faults each need a distinct mitigation. **MCU-03** (excessive watchdog timeout) is mitigated by **(F)** bounding the hardware watchdog to $T_{\mathrm{WDT}} \leq 500\,\mathrm{ms}$, kicked only from a verified-safe state in the main loop so a crash inside an ISR or livelock does not preserve the kick. **MCU-05**

(boot-time output transient) is mitigated by aligning hardware and firmware defaults: **(H)** an external gate pull-down (shared with OUT-02/03) holds the contactor de-energized before firmware configures the GPIO; **(F)** the first firmware action explicitly drives the contactor-control GPIO low. **MCU-08** (ISR race) is mitigated by **(F)** a `volatile`, atomically-accessed state variable with critical sections around multi-step updates, and a one-way latch: once `STOPPED`, only an explicit main-loop reset can clear it.

E. Communications faults (COM)

Six COM faults cover the wireless link between the operator's remote and the E-Stop board: link availability, message integrity, and the RF interface (Table VIII).

TABLE VIII: Communications (COM) faults. Color coding follows Table III.

ID	Fault	L	S	RPN	Mit.
COM-01	Comms link lost, no remote E-Stop	4	3	12	F
COM-02	Noise or spoofed false E-Stop	2	2	4	F
COM-03	Excessive latency, command late	2	4	8	F
COM-04	Packet loss starves control loop	1	3	3	F
COM-05	Protocol mismatch, valid ignored	2	3	6	F, D
COM-06	Radio module or antenna fails	3	4	12	H, D

COM-01 (loss of link) is mitigated by a fail-safe heartbeat rather than direct link-failure detection. **(F)** The remote transmits a fixed-rate heartbeat; if

$$t_{\text{now}} - t_{\text{last_rx}} > T_{\text{link}}, \tag{3}$$

the firmware autonomously asserts Category 0, with $T_{\text{link}} \leq 1\,\text{s}$ balancing nuisance trips against hazard exposure. As with BTN, absence of a positive signal is the failure indicator, so any radio-chain failure produces the same fail-safe response without diagnosing which subsystem failed. **COM-06** (radio/antenna failure) is addressed by **(H)** a single-mate keyed connector for the external receiver: a damaged module, broken antenna, or unplugged module all prevent the heartbeat from establishing, so the same COM-01 fail-safe path also covers a non-functional receiver pre-launch – no separate RF diagnostic needed.

F. HMI / indicators (HMI)

Three HMI faults were identified; none reached the High band (Table IX), since indicator failures compromise the operator's understanding of system state rather than the vessel's autonomous safety functions, which operate without operator intervention.

R7 (diagnostic visibility) motivates this subsystem. **(H)** An addressable RGB LED strip on a single GPIO gives a finite, color-coded vocabulary (green armed, red asserted, amber blink fault, white boot); color-plus-pattern encoding reduces the consequence of partial LED failure or color-blindness [13].

TABLE IX: HMI / Indicators (HMI) faults. Color coding follows Table III.

ID	Fault	L	S	RPN	Mit.
HMI-01	LED shows wrong state, operator misled	2	4	8	H, F
HMI-02	Buzzer fails to sound on E-Stop	1	4	4	H
HMI-03	Indicator pattern ambiguous	4	2	8	F, D

(F) A power-on self-test cycles every state at startup. **(D)** A legend on the enclosure lid and in the quick-start guide removes reliance on operator memory (HMI-03).

G. Connectors / wiring faults (CON)

Five CON faults cover the user-facing interfaces: power input, E-Stop loop, receiver socket, contactor drive lines, and telemetry link (Table X). With the board factory pre-assembled, the entire CON failure surface lives at the connector mating to external harnesses.

TABLE X: Connectors and Wiring (CON) faults. Color coding follows Table III.

ID	Fault	L	S	RPN	Mit.
CON-01	Connector backs out, intermittent contact	4	3	12	H
CON-02	Wires swapped, "stop" becomes "run"	3	4	12	H
CON-03	Floating ground, unpredictable outputs	3	4	12	H
CON-04	Cable shield not terminated to ground	3	2	6	H
CON-05	Strain relief inadequate, fatigue	3	3	9	H, D

The three high-band faults share one architectural mitigation: **(H)** physically incompatible, keyed connector families per interface class (power, loop, receiver, contactor, telemetry). This eliminates CON-02 by construction (a cable either fits the right port or no port), and CON-01/CON-03 by using locking connectors with positive retention and by carrying signal and return together in the same housing, so a mate either establishes both or neither. **(D)** For CON-05, the manual requires strain relief within $100\,\text{mm}$ of the connector body on every external harness.

H. Environmental faults (ENVR)

Six ENVR faults cover moisture, corrosion, vibration, thermal cycling, UV, and fouling (Table XI). The board sits in its own IP-rated enclosure, itself inside the vessel's IP67 compartment, so environmental threats reach it only through cumulative seal failure of two independent enclosures.

ENVR-02 (salt-fog corrosion) is mitigated principally by the double-enclosure architecture; as defense-in-depth, **(H)** external connectors use gold-plated contacts, and **(D)** the manual specifies regular seal inspection and a contact-resistance check. **ENVR-05** (UV degradation) is mitigated entirely by the double-enclosure architecture – the board is never exposed to UV during normal operation, so this fault drives no board-level design decision.

TABLE XI: Environmental (ENVR) faults. Color coding follows Table III.

ID	Fault	L	S	RPN	Mit.
ENVR-01	Water enters enclosure	2	4	8	H
ENVR-02	Salt fog, connector corrosion	3	4	12	H, D
ENVR-03	Vibration cracks solder joints	3	3	9	H
ENVR-04	Thermal cycling, parameter drift	2	3	6	H
ENVR-05	UV degrades coating/insulation	3	4	12	H
ENVR-06	Biological fouling	2	2	4	D

I. System-level faults (SYS)

Six SYS faults cover redundancy posture, fail-safe defaults, and self-test coverage (Table XII).

TABLE XII: System-Level (SYS) faults. Color coding follows Table III.

ID	Fault	L	S	RPN	Mit.
SYS-01	Single-point failure, no redundancy	3	3	9	H
SYS-02	Cascading reset, unsafe boot default	2	3	6	H, F
SYS-03	Power-off not fail-safe	2	5	10	H
SYS-04	Bypass switch left enabled	2	5	10	H, F
SYS-05	No independent backup E-Stop path	1	5	5	D
SYS-06	POST does not verify all paths	3	3	9	F

Both high-band faults are catastrophic ($S = 5$) and both are addressed architecturally. **SYS-03** (power loss leaves contactor energized) is the single most important fail-safe property: **(H)** the contactor coil requires the board to *actively* drive current to energize it, so loss of power, MCU reset, or any coil-drive interruption returns it to de-energized by spring action – satisfying R4 by construction. **SYS-04** (bypass left enabled) is mitigated by eliminating the bypass entirely: **(H)** no physical bypass switch exists on the production PCB; **(F)** debug paths disabling E-Stop logic are gated behind a compile-time flag unset in release builds.

J. Human factors faults (HUMN)

Ten HUMN faults cover operators, integrators, and maintainers across assembly, configuration, operation, and return-to-service (Table XIII).

TABLE XIII: Human Factors (HUMN) faults. Color coding follows Table III. HUMN-03 is shown at its original rating; factory pre-assembly reduces it to the Medium band (see text).

ID	Fault	L	S	RPN	Mit.
HUMN-01	Operator forgets to arm or reset	3	2	6	D
HUMN-02	Wrong button pressed in emergency	3	4	12	H, D
HUMN-03	Student wires E-Stop incorrectly†	4	4	16	H
HUMN-04	Wrong firmware or config uploaded	2	4	8	H, F
HUMN-05	Operator misreads indicators	3	4	12	D
HUMN-06	No E-Stop test after maintenance	3	3	9	D
HUMN-07	Student modifies firmware, breaks SM	2	5	10	H, F
HUMN-08	E-Stop button physically unreachable	2	5	10	D
HUMN-09	Operator intentionally bypasses	3	4	12	H, F
HUMN-10	No pre-launch checklist used	3	3	9	D

†Original FMEA rating; revised to L=2, S=4, RPN=8 following the factory pre-assembly decision below.

HUMN-03 ($\mathrm{RPN} = 16$ as originally rated) was the highest-RPN fault in the FMEA and the principal driver behind factory pre-assembly. With the board shipped fully assembled and the only user-facing wiring being keyed external connectors (§G), likelihood of student-induced internal miswiring drops from *Likely* ($L = 4$) to *Unlikely* ($L = 2$), reducing RPN to 8 (Medium). **HUMN-02** (wrong button under stress) is mitigated by **(H)** a large red mushroom-head actuator on yellow, clearly distinct from other controls, per ISO 13850's actuator spec [1], and **(D)** a requirement that no similarly shaped switch be installed within operator reach. **HUMN-05** (misread indicators) is the operational counterpart to §F's design-time mitigations; the residual fault is mitigated **(D)** by the same enclosure-lid legend. **HUMN-07** (firmware modification breaks E-Stop) is mitigated by **(H)** a recessed USB programming port and **(F)** a separate, non-user-modifiable E-Stop state-machine module loaded at the factory. **HUMN-08** (button unreachable) is an integration-time fault mitigated **(D)** by a mounting-position and 270°-visibility requirement, verified at pre-launch. **HUMN-09** (intentional bypass) is mitigated by removing the means: **(H)** no hardware bypass (SYS-04); **(F)** no runtime command disables E-Stop, and only a power-cycle clears a latched state.

IV. Validation Strategy

The V1 prototype was field-deployed at the 2026 RoboBoat competition, where the core safety functions – normally-closed button loop, heartbeat-based link supervision, Category 0 cutoff, fail-safe default on power loss – operated correctly throughout with no safety-relevant failures, establishing the viability of the architectural primitives carried into V3.

Two V1 findings drove specific V3 changes. First, V1 sensed input voltage and reported it to the operator's PC but implemented no firmware-level threshold response – the operator got a warning, but no autonomous Category 0 cutoff fired when the rail crossed the MCU's safe-operating threshold. PWR-02 was therefore the highest-RPN fault entering V3, now closed by the firmware threshold-crossing logic in §A. Second, V1's single-MCU architecture cohabited E-Stop logic with actuator control and comms on one Arduino Mega; under elevated CPU load the firmware would trigger nuisance E-Stops as a load-induced fail-safe. V3 allocates the E-Stop function to a dedicated MCU on the E-Stop board, sharing no execution context with the ESC-drive/receiver/mission-comms processor, eliminating the load-coupling pathway.

V3 validation is a structured bench-test campaign targeting the mitigations introduced since V1. The MOSFET driver

stage will be exercised at switching frequencies up to several kilohertz from a signal generator, with contactor coil current monitored to verify the POST feedback path (OUT-09) under nominal and abnormal profiles. Noise immunity will be evaluated by injecting common-mode and differential noise on the button loop, heartbeat-input line, and voltage-sense ADC trace, with success defined as no false E-Stop below expected operational noise levels and prompt detection of genuine E-Stop conditions under noise. Brownout response (PWR-02) will be characterized by ramping V_{IN} slowly through V_{th} (Eq. (2)) and confirming Category 0 asserts before the MCU loses control of its outputs. Each test traces to one or more high-band faults from §III; per Table III's post-mitigation criterion, no fault may retain $\mathrm{RPN} \geq 10$ after the mitigations under test are verified.

V. Summary

This appendix has presented a systems-engineering approach to the Emergency-Stop PCB, anchored in requirements R1–R7 derived from competition mandates and the educational-kit context. A Failure Modes and Effects Analysis across ten functional categories and 73 fault modes drove the architectural decisions of the V3 design: undetected brownout (PWR-02, $\mathrm{RPN} = 16$) is addressed by a two-stage voltage-sense scheme, and student-induced miswiring (HUMN-03, $\mathrm{RPN} = 16$) is addressed by factory pre-assembly with keyed connectors as the only user-facing interface, reducing that fault to the Medium band. Every high-band fault traces forward to a documented mitigation in hardware, firmware, or documentation, and from there to an acceptance test in the V3 validation plan. Near-term future work is building V3 and executing the bench-test campaign of §IV, followed by field validation at a subsequent RoboBoat or RobotX deployment; longer-term, formal safety-integrity assessment under IEC 62061 or ISO 13849 would extend this qualitative FMEA into a quantitative reliability framework for higher-stakes deployments beyond the educational context.

References

[1] International Organization for Standardization, *ISO 13850:2015 Safety of Machinery – Emergency Stop Function – Principles for Design*, 3rd ed., Geneva, Switzerland, 2015.

[2] RoboNation, *RoboBoat 2026 Team Handbook*, 2025. Available: https://robonation.org/app/uploads/sites/3/2025/10/RoboBoat-2026-Team-Handbook_111125.pdf

[3] RoboNation, *Maritime RobotX Challenge 2026 Team Handbook*, 2026. Available: https://robonation.gitbook.io/robotx-2026-team-handbook

[4] International Electrotechnical Commission, *IEC 60204-1:2016 Safety of Machinery – Electrical Equipment of Machines – Part 1: General Requirements*, Geneva, Switzerland, 2016.

[5] Pilz GmbH & Co. KG, *PNOZsigma Safety Relays – Product Catalog*, 2025. Available: https://www.pilz.com/en-INT/products/relay-modules/safety-relays-protection-relays/pnozsigma-safety-relays

[6] D. García, R. Barber, and M. A. Salichs, "Design and Development of a Wireless Emergency Start and Stop System for Robots," in *Proc. 11th Int. Conf. Informatics in Control, Automation and Robotics (ICINCO)*, Vienna, Austria, 2014, pp. 223–230.

[7] Georgia Tech Marine Robotics Group, *RoboBoat 2026: Technical Design Report*, Georgia Institute of Technology, 2026. Available: https://robonation.org/app/uploads/sites/3/2026/02/TDR_GTMRG_RB2026.pdf

[8] MIT Arcturus, *RoboBoat 2026: Technical Design Report*, Massachusetts Institute of Technology, 2026. Available: https://robonation.org/app/uploads/sites/3/2026/02/TDR_MITArcturus_RB2026.pdf

[9] Team AMORE, *An Autonomous Surface Vessel for the 2025 RoboBoat Challenge: Technical Design Report*, University of Michigan, 2025. Available: https://robonation.org/app/uploads/sites/3/2025/02/TDR_TeamAMORE_RB2025.pdf

[10] International Electrotechnical Commission, *IEC 60812:2018 Failure Modes and Effects Analysis (FMEA and FMECA)*, 3rd ed., Geneva, Switzerland, 2018.

[11] International Electrotechnical Commission, *IEC 61508:2010 Functional Safety of Electrical/Electronic/Programmable Electronic Safety-Related Systems*, 2nd ed., Geneva, Switzerland, 2010.

[12] J. Ganssle, "Great Watchdog Timers for Embedded Systems," 2004. Available: https://www.ganssle.com/watchdogs.htm

[13] J. L. Burke, R. R. Murphy, M. D. Coovert, and D. L. Riddle, "Moonlight in Miami: An Ethnographic Study of Human-Robot Interaction in Urban Search and Rescue," *Human-Computer Interaction*, vol. 19, no. 1–2, pp. 85–116, 2004.

[14] K. Wang, J. Chu, T. Zhao, and Y. Yuan, "A Safety Analysis and Risk Assessment Method for USV Formation Navigation Mission," in *2025 16th Int. Conf. Reliability, Maintainability and Safety (ICRMS)*, 2025, pp. 364–370.

Appendix E: Design Iterations for UAV ”Kevin”

Mateus Prudencio, Sarthak Aggarwal

I. UAV Design and Development

A. Design Requirements

Early in the design process, the team established the following requirements for the UAV, Kevin:

- 30 min of continuous flight time.
- Reuse ”most” electronics equipment from the previous UAV ”Noodle”.
- Capable of performing competition tasks involving the drone, including any task involving capturing and releasing resource tins.
- Easily disassembled and reassembled for transportation.
- Able to survive a crash from 10 m above the water.
- Able to survive floating in the water for roughly 1 h after a crash before being recovered.

Four design iterations were carried through to physical prototypes before arriving at the current carbon-fiber frame (documented in the UAV Tin Capture Mechanism appendix), each addressing shortcomings identified in the previous build.

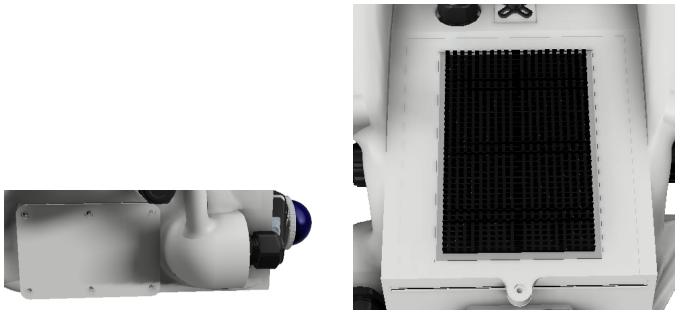
B. Iteration 1



Fig. 1: Iteration 1: fully 3D-printed frame with separate electronics, battery, and capture-mechanism compartments.

This iteration used a fully 3D-printed frame with three distinct sections: an electronics enclosure, a battery box, and the capture mechanism. The electronics box used a large aluminum heat sink to dissipate heat into its surroundings, and the ESCs were mounted on the outside of the drone to further manage heat and keep the electronics enclosure smaller. The bullet AC router was mounted externally in its metal case. For sensing, the drone carried a Mid-360 LiDAR, an Intel RealSense depth camera, and a Raspberry Pi camera. The drone also had multiple access points into the electrical subassembly on the top and sides, shown in Fig. 2.

The primary problem with this iteration was the weight of the UAV. Having separate compartments for the capture mechanism, electrical components, and battery made the design safer and easier to maintain, but significantly added to the overall weight of the vehicle. With this design, flight time would only be around 10–15 min, well below the 30 min requirement.



(a) Side access panel. **(b)** Top heat-sink grille.

Fig. 2: Iteration 1 electronics-enclosure access points.

C. Iteration 2



Fig. 3: Iteration 2: consolidated single-enclosure 3D-printed frame.

Pros:

- Electronics in a more compact area than in the first iteration, leading to a lighter design.
- Propellers have more ground clearance.
- Fully 3D-printed frame allows for rapid prototyping and quick manufacturing times.
- All electronics in one enclosure means no sealing is needed around multiple enclosures.

Cons:

- The 3D-printed frame is still heavy.
- The center of gravity is higher than in the previous iteration.
- Having all electronics in one central compartment makes accessing them for modularity and maintainability more challenging.
- Removing the heat sinks reduces thermal management capability (compensated for with thermal analysis).

D. Iteration 3

Pros:



Fig. 4: Iteration 3: refined 3D-printed frame with a lighter capture mechanism.

- Similar advantages to Iteration 2 from centralizing electronics in one location.
- The more refined capture mechanism significantly reduces weight and complexity.

Cons:

- The design is the least aesthetically refined of the four iterations.
- Following an initial test print, the UAV frame came out much heavier than anticipated, leading the team to scrap the fully 3D-printed frame approach entirely.

E. Iteration 4



Fig. 5: Iteration 4: carbon-fiber frame with rail-mounted electronics – the current design, Kevin.

Pros:

- The fully carbon-fiber frame significantly reduces the weight of the UAV.
- Mounting all electrical components on sliding rails makes maintenance and upgrading/swapping components significantly easier.

Cons:

- Constructing the frame from carbon fiber is a much more time-consuming process that does not allow for many changes once construction is complete.

F. Summary

Across four iterations, the design converged from a fully 3D-printed, multi-compartment frame (Iteration 1) – safe and modular, but far too heavy to meet the $30\,\mathrm{min}$ flight-time requirement – through progressively lighter and more centralized 3D-printed designs (Iterations 2–3), to the current fully carbon-fiber frame with rail-mounted electronics (Iteration 4). The dominant driver across every iteration was weight: each successive design traded some combination of modularity, thermal management, or manufacturing simplicity for reduced mass, ultimately requiring a change in frame material rather than further geometry changes to close the gap to the flight-time requirement. Iteration 4 is the UAV frame carried forward into the tin capture mechanism design documented in the UAV Tin Capture Mechanism appendix.